HEAVY MINERAL ANALYSIS OF SAMPLES FROM THE MISSISSIPPIAN BORDEN GROUP AND DEVONIAN PENDLETON SANDSTONE BED IN SOUTH-CENTRAL INDIANA: IMPLICATIONS FOR SEDIMENTARY PROVENANCE AND DIAGENESIS

A THESIS SUBMITTED TO THE GRADUATE SCHOOL IN PARTIAL FULFILLMENT OF THE REQUIREMENTS

FOR THE DEGREE

MASTER OF SCIENCE

BY

JONATHAN M. VITALI

DR. SHAWN J. MALONE- ADVISOR

BALL STATE UNIVERSITY

MUNCIE, INDIANA

DECEMBER 2019

Table of Contents **Page Number**

ABSTRACT

THESIS: Heavy Mineral Analysis of Samples from the Mississippian Borden Group and Devonian Pendleton Sandstone Bed in South-Central Indiana: Implications for Sedimentary Provenance and Diagenesis

STUDENT: Jonathan Vitali

DEGREE: Master of Science

COLLEGE: Sciences and Humanities

DATE: December 2019

PAGES: 71

The Illinois Basin is a dominantly Paleozoic-aged sedimentary catchment that covers the much of Illinois, southern Indiana, and part of western Kentucky. Analysis of the heavy mineral assemblage of a sedimentary rock offers insight into the origin of this basin's sediments, as well as processes that occur after deposition and burial. In this study, heavy mineral assemblages from nine samples are analyzed. The original purpose of this study was to determine whether the source region of the Illinois Basin was the Appalachians or Canadian Shield. This developed upon the discovery of diagenetic phases to investigate the possible later diagenetic processes based on these authigenic heavy minerals.

One sample was collected from the Devonian-aged Pendleton Sandstone bed, while the rest are from the Mississippian-aged Borden Group, a deltaic sequence present in the Illinois Basin. Petrography and whole rock XRF data indicate a variety of rock types across the sample set. The Borden Group samples are relatively similar, mostly greywacke or siltstones. The outlier

from a petrographic standpoint is the Pendleton Sandstone bed sample, which classifies as a quartz arenite. Elemental data from the SEM was gathered for grains in each sample and tabulated. The same grains were also observed under the petrographic microscope to corroborate the results and identify properties not seen under the SEM. A variety of detrital and authigenic minerals were identified. Zircon, tourmaline, monazite, rutile, anatase, pumpellyite, chlorite, and sapphirine were found throughout the sample set. In addition, authigenic fluorite, pyrite, sphalerite, and glauconite were identified within the Borden samples. The variety of detrital heavy minerals indicates that the Appalachians are the dominant source region for the samples in this study, as the majority of these minerals would have weathered out of the Canadian Shield assemblage, due to its age. Some grains, such as zircons may have Canadian Shield origins, but further study must be done to differentiate them. The presence of pyrite and (its oxidized products from later weathering) indicates an anoxic environment post-deposition, while fluorite, sphalerite and possibly anatase are evidence of metal-rich hydrothermal fluid intrusions. Further study is needed to determine the number of events and composition of the fluids themselves.

I. Introduction

The heavy minerals contained within sedimentary rocks often reflect their sediment source in addition to diagenesis that may have occurred since deposition. Studying these characteristics allows researchers to infer the tectonic history of a given region, as well as differentiate between primary and previously recycled sediment sources (Dickenson et al, 1983). Examples of sediment sources include recycled orogens, continental blocks, and magmatic arcs (Dickenson et al, 1983). Point-counting, age dating of detrital zircon, and heavy mineral analysis are common methods used in tracing the origins of a clastic sedimentary rock. In addition to zircon, other heavy detrital minerals such as monazite, rutile and ilmenite are important indicators of provenance. As weathering occurs during transportation, deposition, and diagenesis, some detrital grains will remain in the rock, which can aid in tracing the sediment's source. Varietal studies that take into account the characteristics of individual mineral grains can further minimize impacts from weathering and alteration (Morton and Hallsworth, 1999).

Diagenesis refers to processes that alter the chemistry of the rock after it is deposited. Factors such as temperature, burial depth, and the initial rock and fluid chemistry determine how diagenesis will proceed (Algeo et al, 1992). For example, carbonates often experience dolomitization, where magnesium replaces calcite in the carbonate sediments. As the chemistry of the grains within the rock changes, inter-grain relationships change as well, often resulting in increased or decreased porosity (Montanez, 1994). Sulfide formation is a common occurrence during diagenesis and can be driven by either biotic or abiotic processes, depending on temperature. Sulfate-reducing bacteria produce sulfur as part of their metabolic process, which combines with ferrous iron to form pyrite (Donald and Southam, 1999). Hydrothermal fluids rich in metals flow through the rock and change mineral chemistry in a process called mineralization

(Pfaff et al, 2011). For example, the iron in pyrite can be replaced by hydrothermally-supplied zinc, resulting in the production of sphalerite. Hydrothermal fluids can originate from magmatic or connate sources (Hall and Friedman, 1963). This process can occur at a range of temperatures (Leach et al, 2010).

This paper analyzes the detrital and authigenic heavy minerals of nine samples collected from the southern and central portion of the Illinois Basin, a sequence of Paleozoic sedimentary rocks that covers the majority of Illinois, southern Indiana, and part of western Kentucky (Figure 1). The basin rests above Proterozoic granitic basement rock, and is comprised of 7,600 meters of sediments that have been deposited and lithified over the past 540 million years (McBride and Kolata, 1999). Much of the data concerning the Illinois Basin has been gathered from hydrocarbon and coal studies (e.g., Damberger, 1971; Bethke, et al, 1991). In addition, detrital zircon provenance studies have examined the eastern and southern portions of the Illinois Basin (Calhoun et al., 2012; Kissock et al., 2015; Thomas et al., 2015; Konstantinou et al, 2015). These detrital zircon studies into the provenance of the Illinois Basin leave two holes in our understanding, however: They are focused on the Pennsylvanian section of the basin, and do not address the portion of the Illinois Basin close to presumed Appalachian sources in southern and central Indiana.

Eight of nine samples taken for analysis belong to the Borden Group, a Mississippian-aged sequence mainly comprised of shales, siltstones, and carbonates (Kepferle, 1977). The Borden Group is described using nomenclature from Ausich et al (1979). The remaining sample is part of the Pendleton sandstone, a bed located at the base of the Devonian-aged Jefferson limestone. This sample is comprised of fine to medium sized sand grains, and is quartz-dominant Droste and Shaver, 1975). The section outcrops at the Fall Creek falls at Fall Creek Park in

Pendleton, Indiana (Shaver et al., 1986). The Pendleton sandstone was sampled in order to constrain the provenance signals from the Borden samples, as well as note any changes in source from the Devonian to the Mississippian. Sediments that formed the Borden Group were transported by rivers originating to the East and Northeast sections of the continent. The Canadian Shield and Appalachian mountains are considered to be the possible sources (Kepferle, 1977); in addition, sediment may be recycled from older sedimentary rocks, although this source is difficult to constrain.

The hypothesis of this study is that if there is a variety of heavy minerals identified throughout the samples, the source will likely be the Appalachians. If there is less of a variety, such as just zircon in the samples, the source may be the Canadian Shield instead. The original objectives of this paper were to; (1) analyze the detrital heavy minerals present in each of the samples to determine whether they originated from the Canadian Shield or Appalachians, (2) analyze authigenic heavy minerals in each sample to make inferences about the diagenetic history of the Borden Group and Pendleton sandstone bed and (3) Describe rock samples based on whole-rock geochemical analysis, to better constrain the host rock characteristics. Due to the abundance of authigenic heavy minerals, relative to detrital heavy minerals, a quantitative provenance analysis was not possible. However, the presence of these minerals opened up a new and interesting avenue of investigation related to their occurrences and what it meant for diagenesis and later mineralization in the Borden Group.

Figure 1. Map showing the location and extent of the Illinois Basin. (Oil and Gas Investments Bulletin)

II. Geological Setting

The Illinois Basin is an oval shaped intracratonic basin that covers approximately 284,900 km^2, covering most of Illinois in addition to parts of Indiana, Kentucky, Tennessee, and Missouri (Figure 1). The basin is filled in with more than 2 km of Paleozoic marine and non-marine strata. Accommodation for this sediment initially developed due to rifting at about 600 Ma and subsequently filled with sediment over the next 540 Ma (McBride and Kolata, 1999).

Tectonic History

Formation of the basin was driven by extension within the North American interior, as evidenced by Precambrian mafic flood basalts with normal faults alongside them (Stewart, 1976). The extension has been linked to the split of Rodinia into Laurentia and Gondwana (Kolata and Nelson, 1990). Heidlauf et al (1986) used well log data and computer modeling to create subsidence curves that represented the rate of subsidence over time (Figure 2). These curves indicated that there were two distinct types of rifting during the formation of the basin: mechanical (fault driven) and thermal (plume driven). For the first 10 Ma, the subsidence curve exhibited a relatively steep slope. However, the slope became much more gradual at the 520 ma mark, an occurrence that was inferred to be caused by change in the force driving the subsidence. It was determined that during the first 10 Ma, subsidence was driven by faulting, after which an intrusion of a mantle plume resulted in thermal-controlled subsidence. Two more distinct events were identified within the subsidence curves, but their origins could not be inferred (Heidlauf et al, 1986).

Stratigraphic and Depositional Sequences

Sediment delivery to the Illinois Basin was often impacted by tectonic events on the Laurentian margin (Kolata and Nelson, 1990), primarily the three major orogenies along the eastern Laurentian margin: The Taconic (Ordovician), related to collisions between Laurentia and volcanic island arcs, the Acadian (late Devonian-early Mississippian), resulting from collisions between Laurentia and several micro-continents, and the Alleghenian (late Mississippian), where Laurentia experienced a terminal ocean basin closure during a continent-continent collision with Gondwana to form Pangaea (e.g. Hatcher, 2010). The basin stratigraphy also reflects multiple sequences of transgression and regression, especially those of the Tippecanoe and Kaskaskia sequences.

The Kaskaskia sequence base in the Illinois Basin is marked by the sandstone layer of the Dutch Creek sandstone and its equivalents, such as the Pendleton Sandstone bed, located above the unconformity with Tippecanoe units marking the base of the Muscatatuck group (Swann, 1963). Carbonate deposition rapidly commenced as sea levels rose and the sediment supply from the Appalachians dwindled, resulting in the deposition of Geneva and Jeffersonville limestones. This pattern changed again in the late Devonian, as sediment eroded from the Acadian Orogeny deposited in the Illinois Basin from a series of river delta systems, forming the Devonian to early Mississippian New Albany Group shales (Ettensohn, 1985). This unit is dominated by green to brownish-black, organic rich shale unit that extends west and southwest of the Cincinnati and Kankakee arches (Shaver et al., 1986). As the deltas prograded from the east-northeast, coarser sediments reached the Illinois Basin to form the Borden Group.

The Borden Group is a deltaic sequence of sicliclastic and carbonate beds that were deposited in the early Mississippian, including the lower New Providence shale, the middle

Spickert Knob Formation, and the upper Edwardsville Formation (Ausich et al, 1979; Shaver et al., 1986; Swezey, 2009). The New Providence Shale is characterized by dark colored, greenish to bluish gray shales with some variably fossiliferous carbonate beds present in areas (Shaver et al., 1986). The contact between the New Providence Shale and the overlying Spickert Knob formation is poorly defined and gradational (Shaver et al., 1986). The Spickert Knob formation represents part of the general coarsening-upward sequence in the Borden Group, likely representing delta slope deposits (Shaver et al., 1986). This unit is dominated by siltstone, with lesser volumes of shale, sandstone and carbonate present (Shaver et al., 1986). The Spickert Knob formation conformably grades into the overlying Edwardsville formation with intertounging units (Shaver et al., 1986). The Edwardsville formation represents the top of the Borden Group. It is dominantly composed of siltstone, sandy shale, and sandstone with some carbonate units in places (Shaver et al., 1986). Figure 5 shows a stratigraphic column of the Borden Group taken from Kepferle (1977), referred to as the Borden Formation in Kentucky (Kepferle, 1977). The formation records deposition in delta platform environments (Figure 6), which show deeper water settings to the southwest (Shaver et al., 1986). In Indiana, the Borden Group outcrops in a northwest-southwest trend, ranging from 485 to 800 feet thick, and up to 38 miles wide (Stockdale, 1939). During this time, the Illinois Basin was covered by a shallow inland sea, supplied by rivers flowing from the east and north (Figure 7) (Kepferle, 1977). Sediments supplied from these river systems likely came from the northern Appalachian province and/or the Canadian Shield.

The majority of the Borden Group is made up of siltstone and shale, with lenses of carbonates and sandstones throughout. Units of limestone and dolostone can be found at the top of the formation, while marine fossils are present throughout the entirety of the group (Kepferle,

1977). Isopach maps of Borden beds indicate east-west progradation (Ausich et al, 1979). Changes in lithology between shale and silt/sandstone are evidence of fluctuating levels of river discharge over time, while the presence of carbonates suggest drier periods where there was a lack of detrital sediment inflow (Sable, 1979). The Floyds Knob limestone bed serves as an example of this occurrence (Ausich et al, 1979).

Kaskaskian sedimentary sequences stratigraphically above the Borden group were deposited throughout the late Mississippian as depositional environments shifted between deltaic systems and carbonate sediments (Swann, 1963; Swezey, 2009). This led to the formation of five more groups above the Borden. The Sanders Group is dominated by carbonate deposits, with small amounts of siliceous material found throughout. The Ramp Creek and Muldraugh Formations are composed mainly of fine-grained limestone and dolomite, with small amounts of shale and siltstone. Moving upward into the Harrodsburg Limestone, bioclastic calcarenites become the dominant rock type. Geodes and chert lenses can also be found throughout the group (Shaver, 1986). The Blue River Group rests conformably atop the Sanders Group, and is also rich in carbonate material. Significant amounts of shale, chert, anhydrite, and gypsum are also found in the group (Shaver, 1986). The West Baden Group consists of the Elwren Formation, Reelsville Limestone, Sample Formation, Beaver Bend Limestone, and Bethel Formation. The dominance of shales and mudstones in this group marks another shift toward increased sediment inflow and local regression into the Illinois Basin (Shaver, 1986), a pattern that continued through the deposition of the Stephensport Group. The grain size indicates that low flow conditions were present at the time of deposition. The Kaskaskia sequence concluded as sea level dropped following the deposition of the Buffalo Wallow Group, a unit dominated by shale, mudstone, and siltstone, with areas of sandstone and limestone beds (Shaver et al., 1986).

Figure 2. (a) Tectonic subsidence curve showing the rate of subsidence over time, as well as the transition to thermal subsidence. (b) Cross section diagram of the Illinois Basin showing the amount of subsidence for the thermal and mechanical phases, as well as tell-tale thermal bulges on the left and right flanks. Points D, S, and F represent the wells where data was collected (Heidlauf et al 1986).

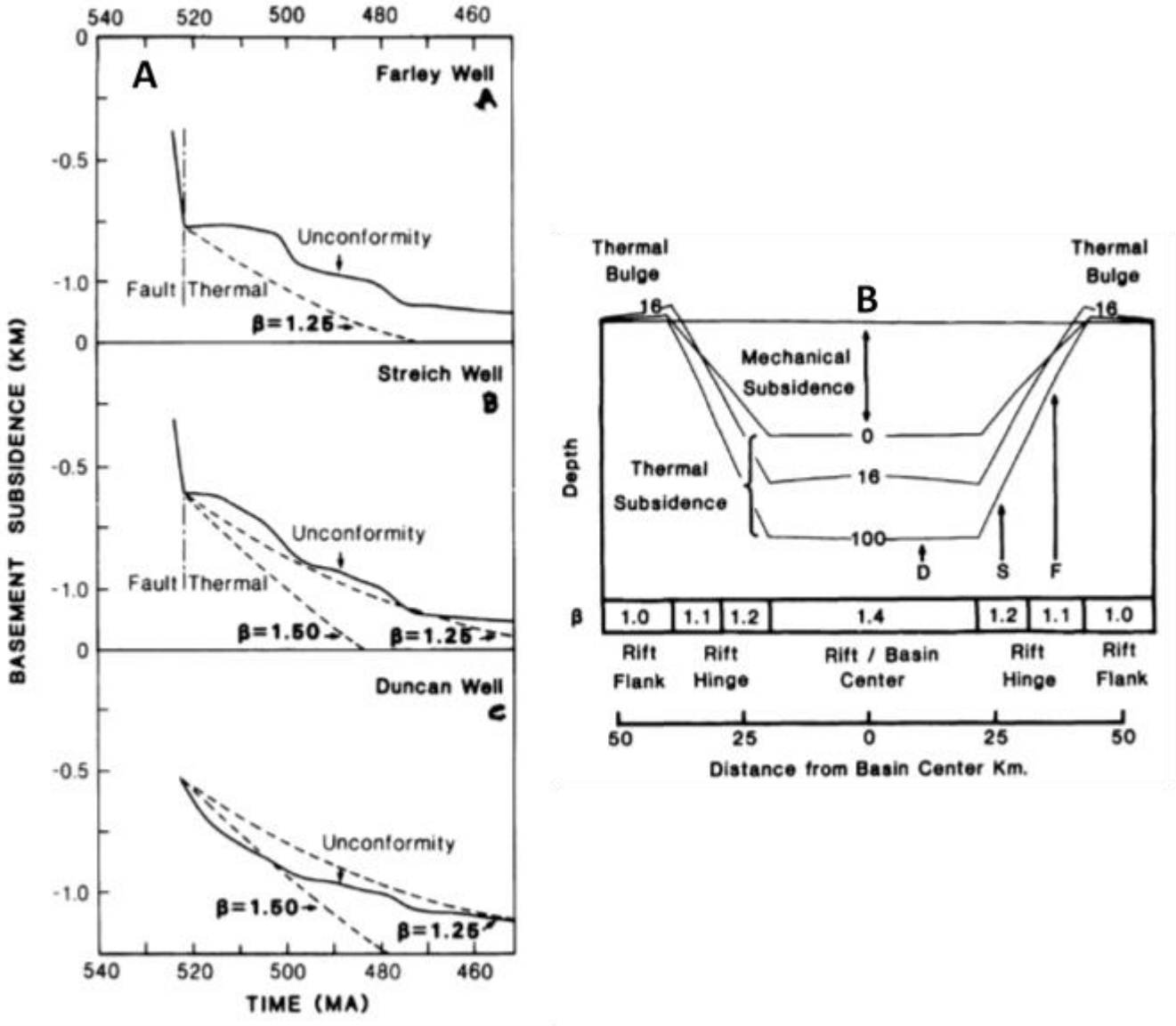

Figure 3. Simplified geological map of the eastern Illinois Basin of Indiana, showing the sample locations in the Illinois Basin. Map generated by data available from the USGS and Google Earth.

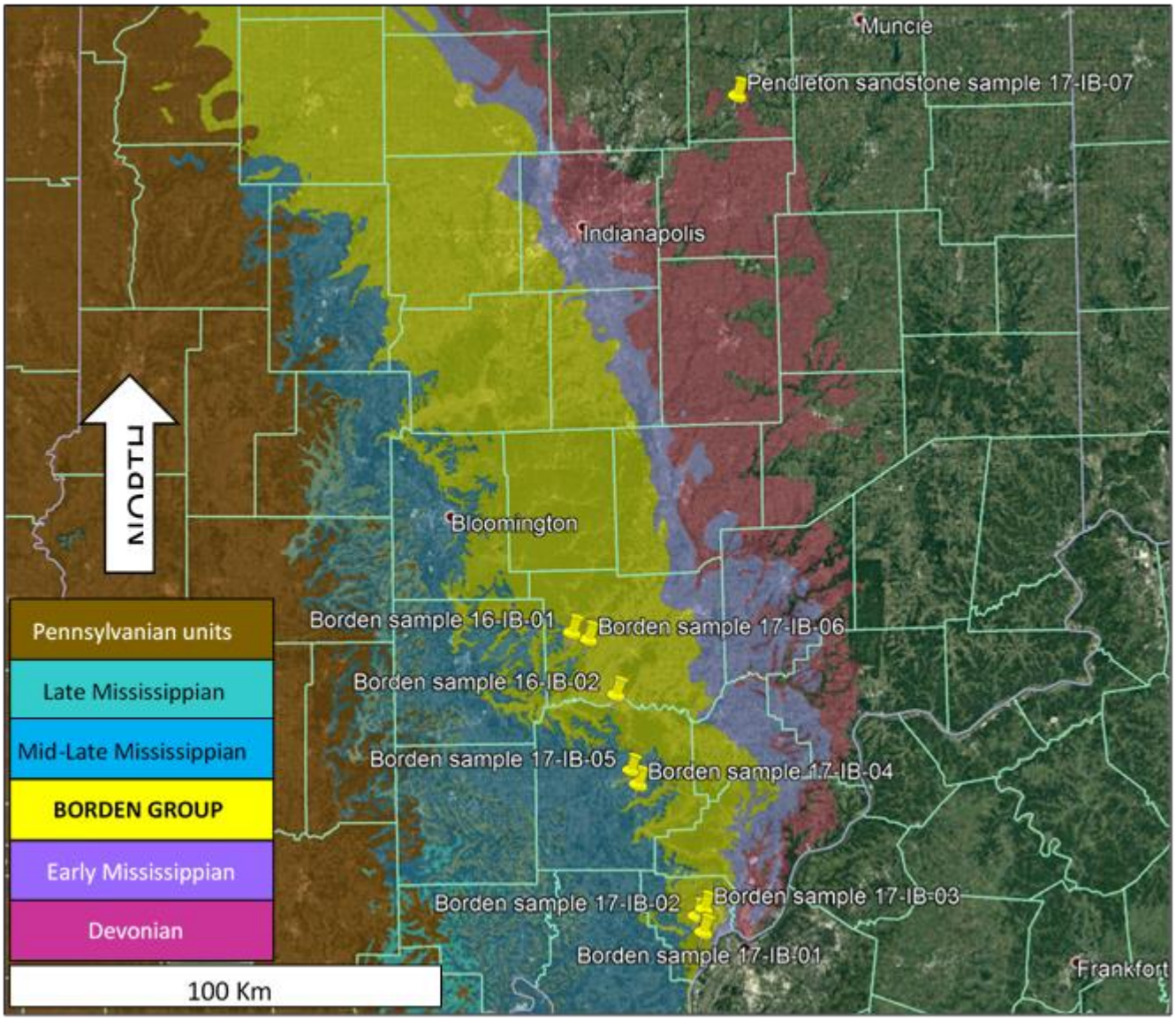

Figure 4. Generalized stratigraphic column of Indiana bedrock, including the major Illinois Basin forming units. The Borden Group interval is highlighted in the red rectangle. Adapted from Thompson et al., (2010).

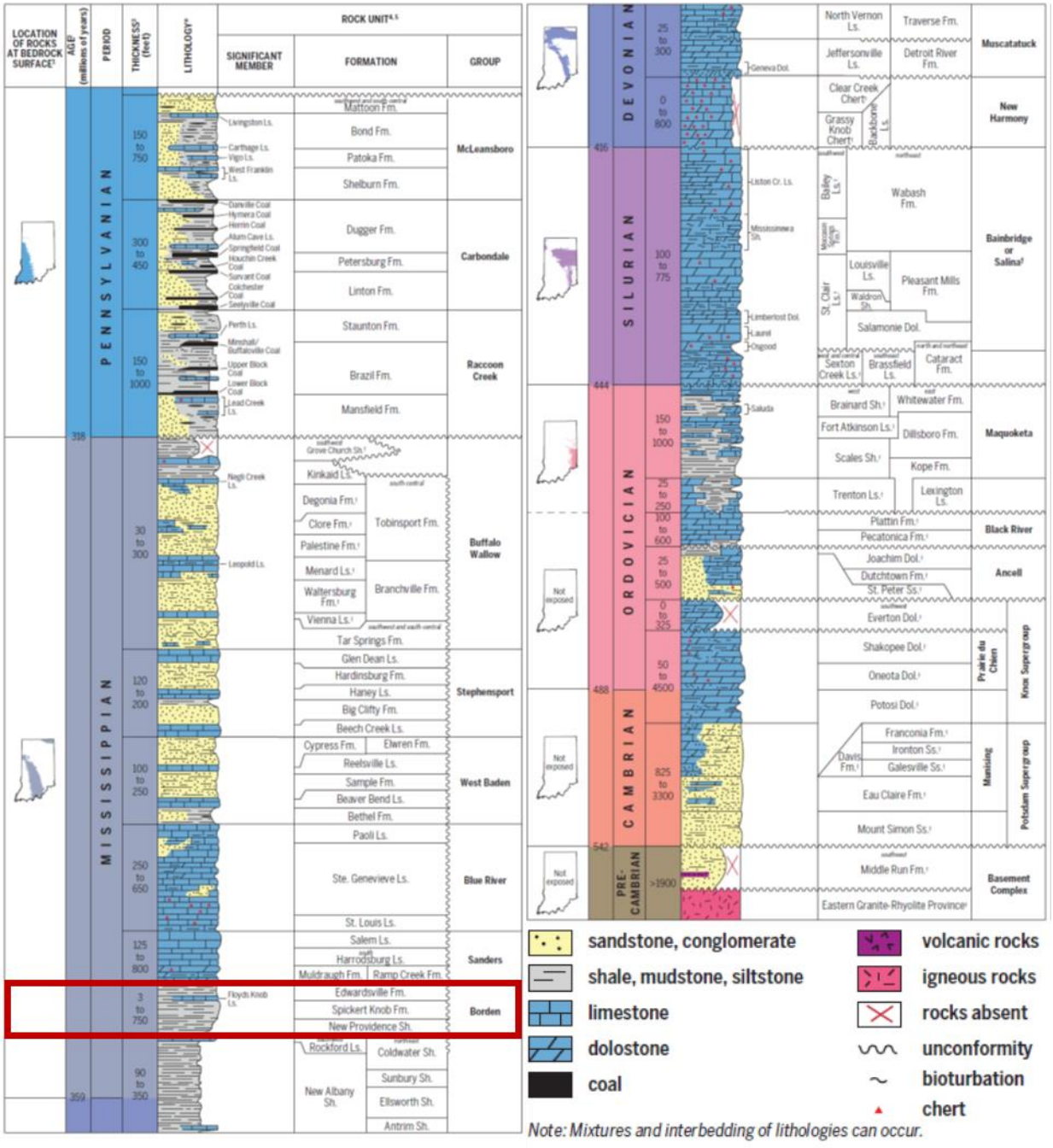

Figure 5. Stratigraphic column of the Borden Formation in western Kentucky. It is synonymous with the Borden Group of southern Indiana, with the exception of the Floyds Knob bed being grouped into the Edwardsville Formation in the Borden Group. Figure taken from Kepferle (1977).

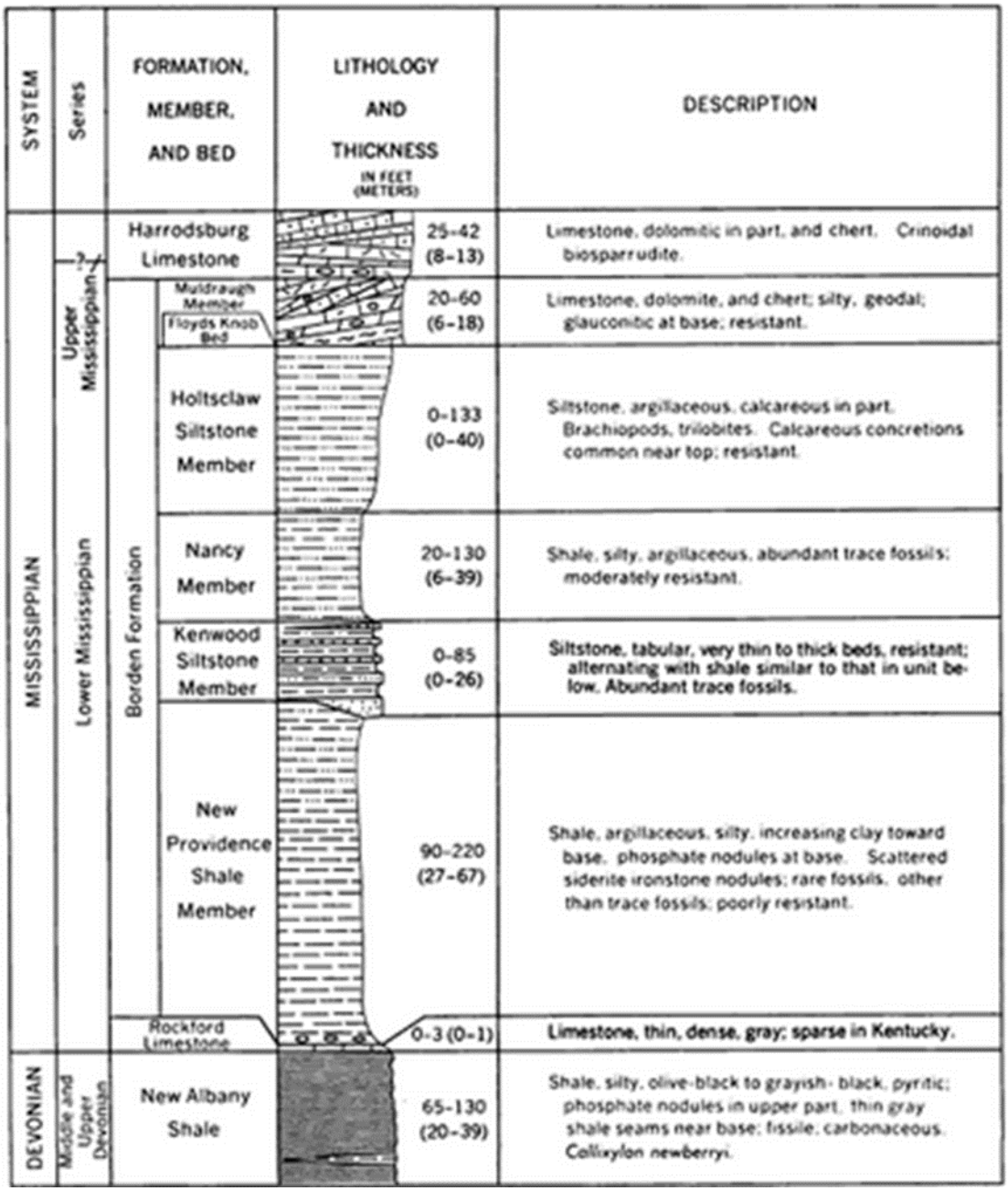

Figure 6. North-South cross section of early to middle Mississippian lithostratigraphic units from southern Indiana to northern Kentucky. Taken from Ausich et al., 2018.

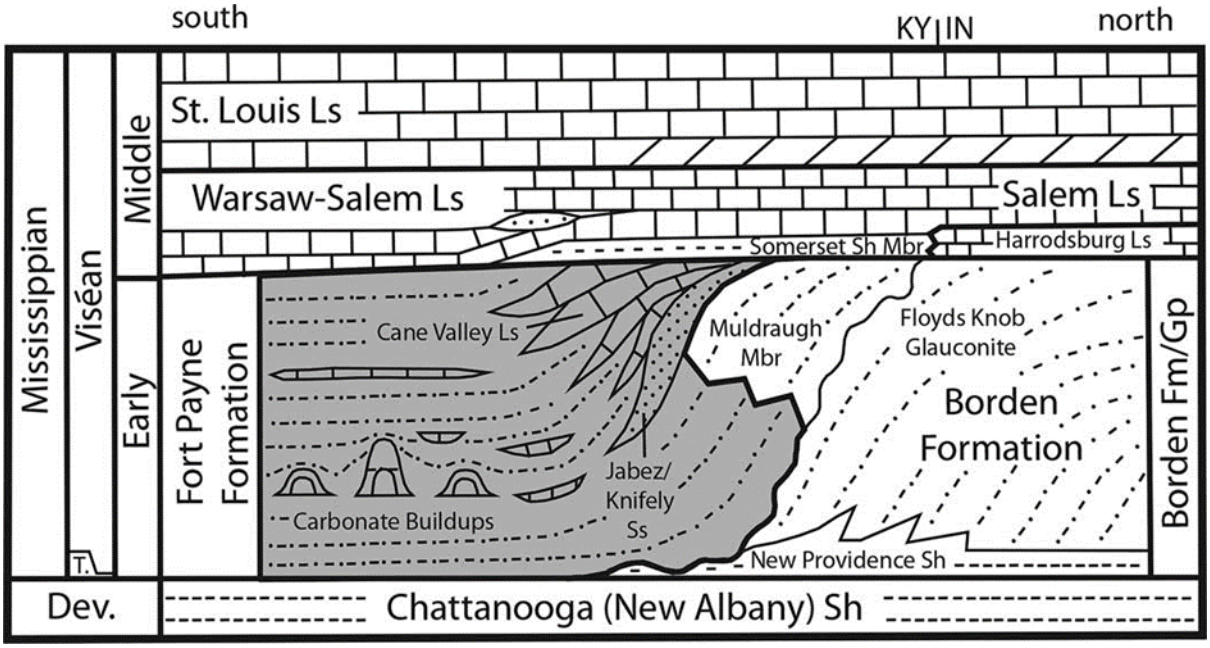

Figure 7. Map showing paths of Mississippian rivers that supplied the Illinois Basin with sediment. The rivers flowed from east-northeast sources, originating in the Appalachian Mountains and Canadian Shield regions respectively (Kepferle, 1977).

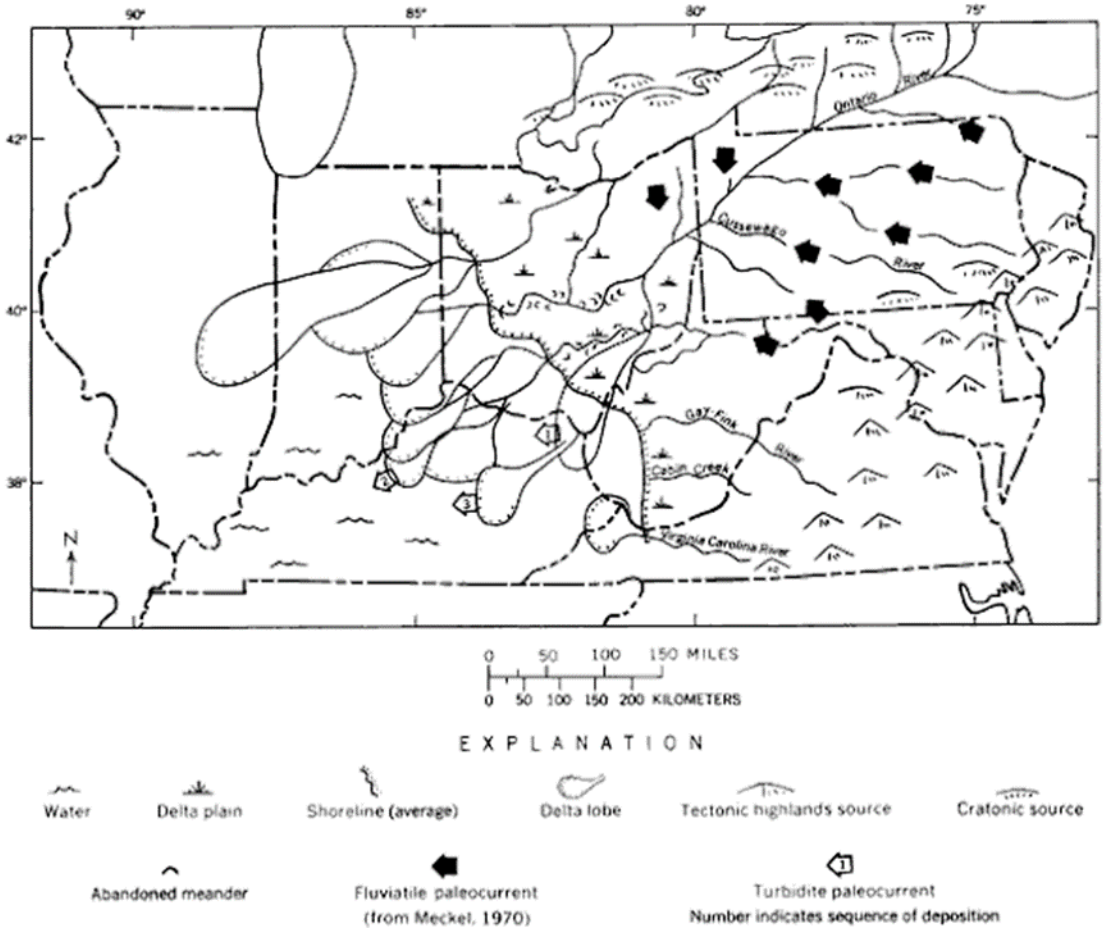

III. Methods

Sample Collection

Nine samples were collected from sites located in the Eastern portion of the Illinois Basin of Indiana: eight samples were collected from siltstone outcrops of the Mississippian-aged Borden Group, and one from the Pendleton Sandstone bed at the base of the Jefferson limestone (Figure 3). Potential sample locations were chosen using geologic maps from the Indiana Geological Survey and Google Earth to determine where outcrops were located. Samples were collected where outcrop was safely accessible, generally from road cut exposures. Rock hammers were used to obtain relatively unweathered samples of each outcrop. GPS readings and pictures were taken at each site for the purpose of future reference and map generation. Samples were then stored in labeled containers and transported to the lab for preparation.

Mineral Separation

Once in the lab, hand sample descriptions were performed before the samples were cut into smaller fragments for thin section preparation and further processing. A large aliquot of each sample was crushed with a Bico Chipmunk crusher, and pulverized using a Bico UA Pulverizer at Ball State University. The pulverized sample was then poured through a 20 Φ sieve to remove unpulverized rock fragments from the sample. The grains smaller than 20 Φ were then poured onto a Gemeni Water table in order to separate mineral grains by density. Denser mineral grains are trapped in the table's grooves and moved down to collection bags, while less dense grains (e.g., feldspars and quartz) are washed into the sides of the table and collected separately.

After being run through the Gemini table, vacuum filtration was performed on the contents of each bag in order to drain as much water out as possible. Ethanol was poured through

the samples in order to further facilitate water removal, as the alcohol displaces water from the sample and evaporates more quickly. Lastly, the samples were set to dry in an oven set at 75 ^{0}C for two days totally dry the sample.

Standard heavy mineral separation using bromoform (density = 2.89 g/mL) was performed to further purify a heavy minerals separate. Samples were then put through a Frantz magnetic separator set between 0.2 and 0.5 amps in order to remove the most magnetic particles, generally metal from the disk mill process. Residual calcite was removed by a 10 percent hydrochloric acid solution rinse. The samples were then sieved through 355 micron mesh to further filter for finer grain sizes, which typically includes more heavy minerals. Grain mounts were made by first pouring the sample onto double-sided 3M #410M tape within a pre-cut template. Two samples were loaded onto each mount; in addition, pure quartz was added next to the samples in order to gauge thickness during thin section polishing. A 2.5 cm ring mount was placed over the sample and Buhler Epo-Tek 301 epoxy was added. The epoxy was left to cure for 24 hours. Once cured, the samples were polished using 600 and 2500 grit sandpaper and subsequently cut to approximately 3 mm thickness prior to observation under a Hitachi TM-1000 desktop Scanning Electron Microscope (SEM) system. Once SEM observation was completed, the samples were epoxied to glass slides and polished into thin sections using the Hillquest Thin Section Machine, in the sample preparation lab at Ball State University.

Sample Analytical Methods

In addition to hand sample descriptions, analysis was conducted via SEM, petrographic microscope, and x-ray fluorescence (XRF). An aliquot of each sample was also ground into a fine powder with a mortar and pestle, then pelletized in preparation for XRF analysis using the Thermo QuanX EC X-ray Fluorescence Machine at Ball State University. Compressed pellets

for XRF analysis are prepared by the following process. 9 to 10 g of each sample powder was then weighed, and put into a weighed ceramic crucible. This aliquot was then poured into a plastic ceramic mixing cup, where polyvinyl alcohol (PVA) was added to make the mixture more saturated and homogenous. The PVA solution used 5 g of dried, 85-90% hydrolyzed grains and 95g (95 mL) 18Ω deionized water. The mixture was then heated and stirred until the PVA grains dissolved. Nineteen drops of PVA were added into the 8 g of each aliquot, and then mixed until homogenized. The material was placed into a pellet press apparatus, and pressed at 2-10 tons/in2 for 5-10 sec over three minutes. The pellets were then extracted and set to dry in a Fisher Scientific Isotemp Oven at 50˚C.

For the SEM portion, sections of each sample were photographed with the Hitachi TM-1000 SEM and put together in PowerPoint in order to create a physical map of the sample figure. Images were taken in Back-scattered electron (BSE) mode, and elemental spectra were collected using the Energy Dispersive Spectroscopy (EDS). For each sample, four bulk elemental spectrum readings were generated, where large portions of the sample were placed under the electron beam at once in order to obtain a general geochemical makeup of the sample before selecting individual grains. Next, twenty grains from each sample were randomly selected and individually analyzed for their elemental spectrum. Each grain was circled and numbered on the map for future reference.

Thin sections and grain mounts were examined using a Nikon Eclipse LV100NPOL petrographic microscope, with a Nikon DS-Fi2 camera attached. Grains selected during the SEM phase were observed in order to better constrain their mineralogy. *Heavy Minerals in Colour*, by Mange and Maurer (1992) as well as *A Colour Atlas of Minerals in Thin Section* by MacKenzie and Guilford (1980) were used as references in this step to ensure correct optical identifications.

Due to the paucity of detrital heavy minerals, quantitative methods such as ribbon counting would not yield a statistically useful result. Instead, each identifiable non-opaque phase was identified and counted.

IV. Results

The following section reviews the overall results of the study. Full details and additional supporting figures are presented in Appendicies A-C.

Whole Rock Characterization

The results of the sample petrography and XRF analysis are detailed below, sample by sample. Table 1 summarizes the XRF geochemical data for the samples.

Sample 16IB01. This sample is grey in color, exhibits light/dark layering, has silt-sized grains, and what appear to be fossil fragments. The sample fizzes when exposed to HCl. Three major geochemical constituents are SiO_2 (76.3%), Al_2O_3 (8.90%), and CaO (6.28%). This is consistent with the observed quartz and clay minerals.

Sample 16IB02. This sample has a light brown weathered face, tan fresh face, and is composed of fine-grained sand. Three major geochemical constituents are SiO_2 (89.0%), Al_2O_3 (12.52%), and Fe_2O_3 (2.23%). This is consistent with the observed quartz and clay minerals.

Sample 17IB01. This sample is tan in color, with rust stains on the weathered face, and is made up of silt-sized grains. Geochemical parameters reveal that it is geochemically composed of CaO (48.77%), MgO (11.79%), and SiO_2 (9.4%). However, the results for this sample are suspected to be erroneous as it does not fizz with HCl, as expected with a rock with a high CaO content.

Sample 17IB02. This sample is grey in color, with a weathered face has a brownish tint to it. It is made up of silt-sized grains. Three major geochemical constituents are SiO_2 (77.8%), Al_2O_3 (18.53%), and MgO (3.59%). This is consistent with the observed quartz and clay minerals.

Sample 17IB03. This sample is grey in color, while the weathered face shows darker grey staining. It is made up of silt-sized grains. Three major geochemical constituents are SiO_2 (78.1%), Al_2O_3 (14.46%), and Fe_2O_3 (4.78%), consistent with the observed quartz and clay minerals.

Sample 17IB04. This sample is tan in color, with a weathered face that is dark brown in places. It contains microfossils, and fizzes when exposed to HCl. Three major geochemical constituents are SiO_2 (41.9%), CaO (24.67%), and MgO (6.29%). This is consistent with the mixed silty and clay rich matrix with abundant fossil fragments.

Sample 17IB05. This sample has a light grey fresh face and a dark grey to rusty brown weathered face. Microfossils are present, and the sample fizzes when exposed to HCl. The sample is made up of silt-sized grains. Three major geochemical constituents are SiO_2 (73.2%), Al_2O_3 (17.51%), and Fe_2O_3 (7.07%); however, the low CaO (0.22%) indicated by the chemical analysis is not consistent with strong HCl reaction. The reason for this discrepancy may be due to the mismatched igneous standards we were forced to use during XRF analysis.

Sample 17IB06. This sample is light grey in color, and composed of silt-sized grains. Three major geochemical constituents are SiO_2 (71.4%), Al_2O_3 (18.38%), and Fe_2O_3 (6.15%). This is consistent with the observed quartz and clay minerals.

Sample 17IB07. This sample is white in color with rust stains, and is composed of very poorly cemented, fine to medium sand grains. Three major geochemical constituents are SiO_2 (92.9%), $A1_2O_3$ (1.20%) and CaO (0.67%). This is consistent with the superabundance of quartz grains observed in the sample.

Heavy Mineral Analysis

Sample 16IB01. Several heavy minerals were identified in this sample. Pyrite was identified based on SEM elemental data combined with the grains' opaque characteristics under the optical microscope. Glauconite was identified for its dark green coloration under plane polarized light. Tourmaline was identified due to its elongated hexagonal shape, brown to dark brown pleochroism, interference colors, and extinction angle. Zircon was identified based on its high relief, elongated shape and interference colors. Rutile was identified due to its distinct dark brown color under plane polarized light, as well as having high amounts of titanium from the SEM data. Monazite was identified by its interference colors as well as the presence of cerium found in the same grain under the SEM.

Sample 16IB02. Tourmaline was identified based on its shape and interference colors. Rutile was identified based on its distinct brown coloration under plane polarized light and supplemented by SEM elemental data. Fluorite was identified based on its characteristic negative relief.

Sample 17IB01. Pyrite was identified based on its opaque appearance and supplemented by SEM elemental data revealing large sulfur and iron components. Fluorite was identified based on its characteristic negative relief. Zircon was identified based on its high relief in addition to its interference colors and extinction angle. Sphalerite was identified based on the corresponding grains' "dusky" appearance as well as data from the SEM indicating the presence of zinc and iron in these grains.

Sample 17IB02. Pyrite was identified based on its opaque appearance in addition to SEM elemental data showing large amounts of sulfur and iron in the grains. Zircon was identified

based on its high relief, interference colors and parallel extinction angle. Pumpellyite was identified based on its fibrous green appearance, yellowish green to bluish green pleochroism, Tourmaline was identified based on its elongated hexagonal shape, interference colors, and medium relief. Fluorite was identified based on its negative relief and isotropic nature under cross polarized light.

Sample 17IB03. Pyrite was identified based on its opaque appearance in addition to SEM elemental data showing significant amounts of sulfur and iron in the corresponding grains. Zircon was identified based on the corresponding grain exhibiting 2nd order blue, purple, and yellow under cross-polars. Colors were arranged in a zoning pattern. Medium to high relief was also observed.

Sample 17IB04. Opaque grains were determined to be pyrite and sphalerite, based on SEM elemental data revealing both iron-sulfur and zinc-sulfur compositions. Chlorite was identified based on its green color under plane polarized light, in addition to its relief. Zircon was identified based on its interference colors as well as its high relief. Fluorite was identified based on its negative relief and isotropy. Glauconite was recognized as small, green flecks that were almost opaque under plane polarized light.

Sample 17IB05. Opaque grains were believed to be pyrite, based on SEM elemental data. A possible chlorite grain was identified based on dark grey/ blue birefringence, with no visible structures or cleavage in the grain.

Sample 17IB06. Opaque grains were believed to be pyrite, based on SEM elemental data. Fluorite grains were identified based on their negative relief. Pumpellyite was identified based on

its green color and radiating, fibrous nature. Chlorite was identified based on its green, non-fibrous appearance. It also exhibited dark bluish coloration under crossed polars.

Sample 17IB07. Zircon and rutile grains were abundant, identified by the properties described above. Fluorite grains were also present, as evidenced by their negative relief and isotropy under crossed polars. Sapphirine grains were identified by a number of factors. They were oval shaped and blue under plane polarized light. They lacked pleochroism and cleavage, and exhibited dark blue to black coloration under crossed polars, almost appearing isotropic. Anatase was identified based on its high relief and SEM data revealing a composition of 75% Ti, 18% Si, and 7% Al. The distinct rectangular shape of this particular grain indicate that it may be authigenic, as the majority of the grains in the sample are well-rounded.

Table 1. XRF geochemical results in major element oxide form. The presence of a dash in the cell indicates that no data could be gathered for that oxide in the sample.

Analyte	17IB01	17IB02	17IB03	17IB04	17IB05	17IB06	17IB07	16IB01	16IB02
SiO_2	9.4	77.8	78.1	41.9	73.2	71.4	92.9	76.3	89.0
TiO_2	-	1.23	1.29	0.36	1.14	1.16	0.04	0.79	2.09
Al_2O_3	1.61	18.53	14.46	6.17	17.51	18.38	1.20	8.90	12.52
Fe_2O_3*	0.43	4.78	3.48	3.78	7.07	6.15	0.22	2.17	2.23
MnO	0.01	0.03	0.03	0.07	0.04	0.03	0.00	0.04	0.04
MgO	11.79	3.59	2.31	6.29	2.40	2.67	0.19	1.24	0.90
CaO	48.77	0.83	0.78	24.67	0.22	0.29	0.67	6.28	0.09
Na_2O	0.38	2.46	2.19	0.70	2.37	1.62	0.00	1.15	2.18
K_2O	1.00	2.57	2.29	1.89	2.92	2.91	0.05	1.34	1.22
P_2O_5	-	0.12	0.06	-	0.19	0.02	0.01	0.03	0.15

Table 2. Table showing the distribution of detrital heavy minerals in in each sample. A green X shows that the mineral was positively identified.

Sample ID	Pumpellyite	Chlorite	Tourmaline	Zircon	Rutile	Anatase	Monazite	Sapphirine
16IB01			X	X	X		X	
16IB02				X	X			
17IB01				X				
17IB02	X		X	X				
17IB03				X				
17IB04		X		X				
17IB05		X						
17IB06	X							
17IB07				X	X	X		X

Figure 8. Photograph of sample 16IB01 showing tourmaline, monazite and opaque grains taken at 40x magnification. The opaque grains are likely to be pyrite, based on SEM elemental data. In addition to optical properties, the monazite was also identified in part by SEM elemental data. Photo by Jonathan Vitali.

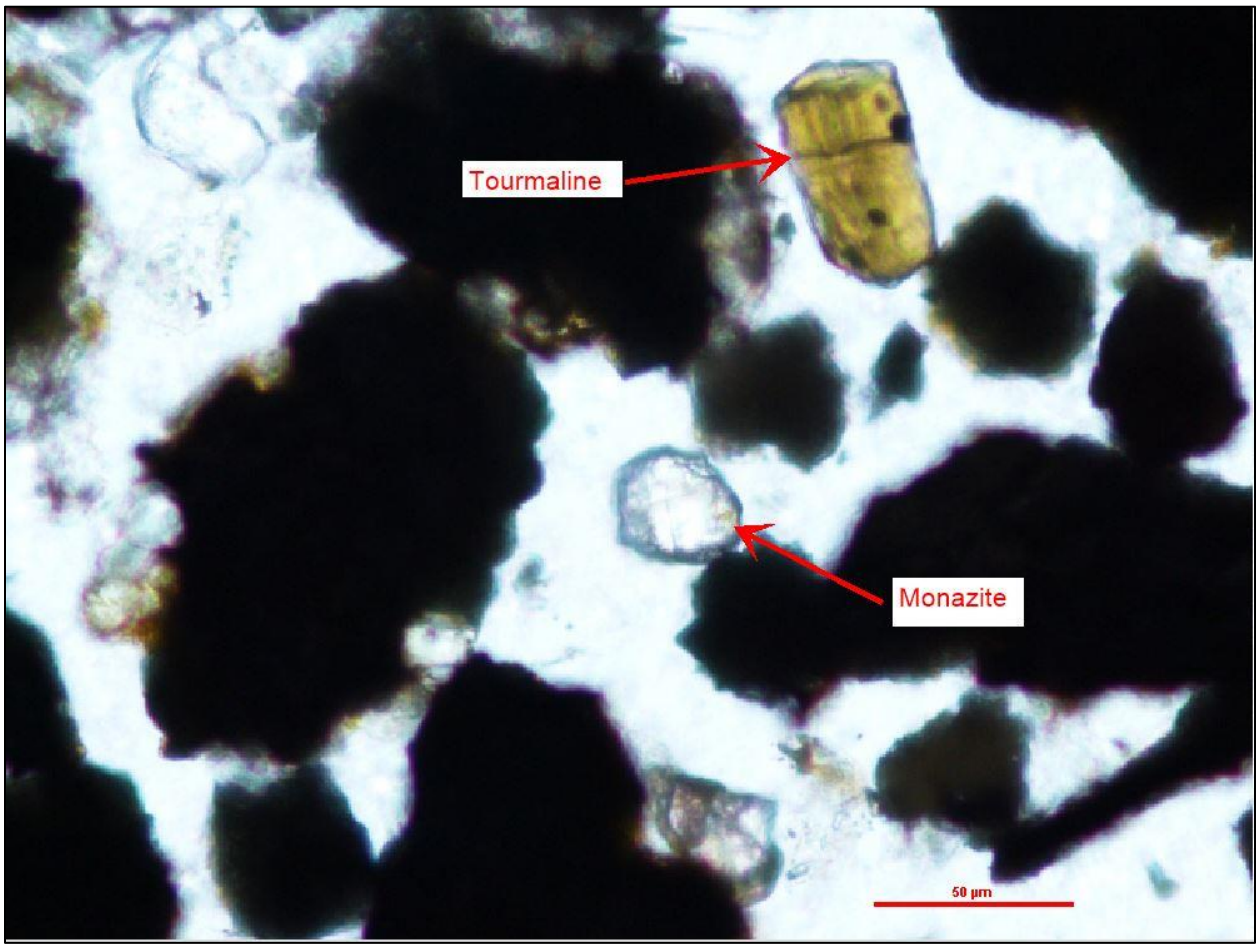

Figure 9. Photograph of sample 16IB02 showing zircon, rutile, and tourmaline grains at 20x magnification. Photo by Jonathan Vitali.

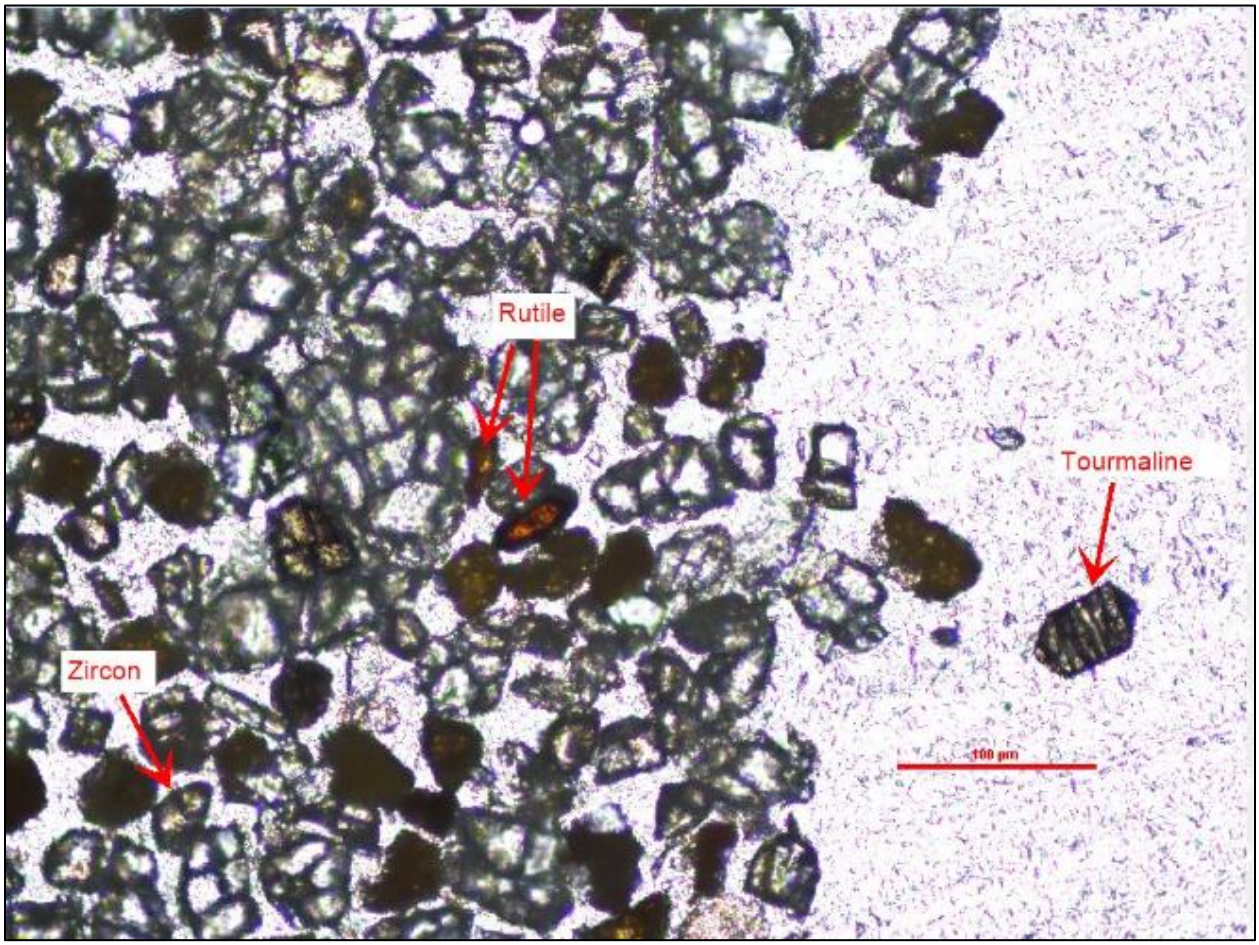

Figure 10. Photograph of sample 17IB01 showing a zircon grain surrounded by opaque and gray "dusky" grains that are likely pyrite and sphalerite, respectively. Photo by Jonathan Vitali.

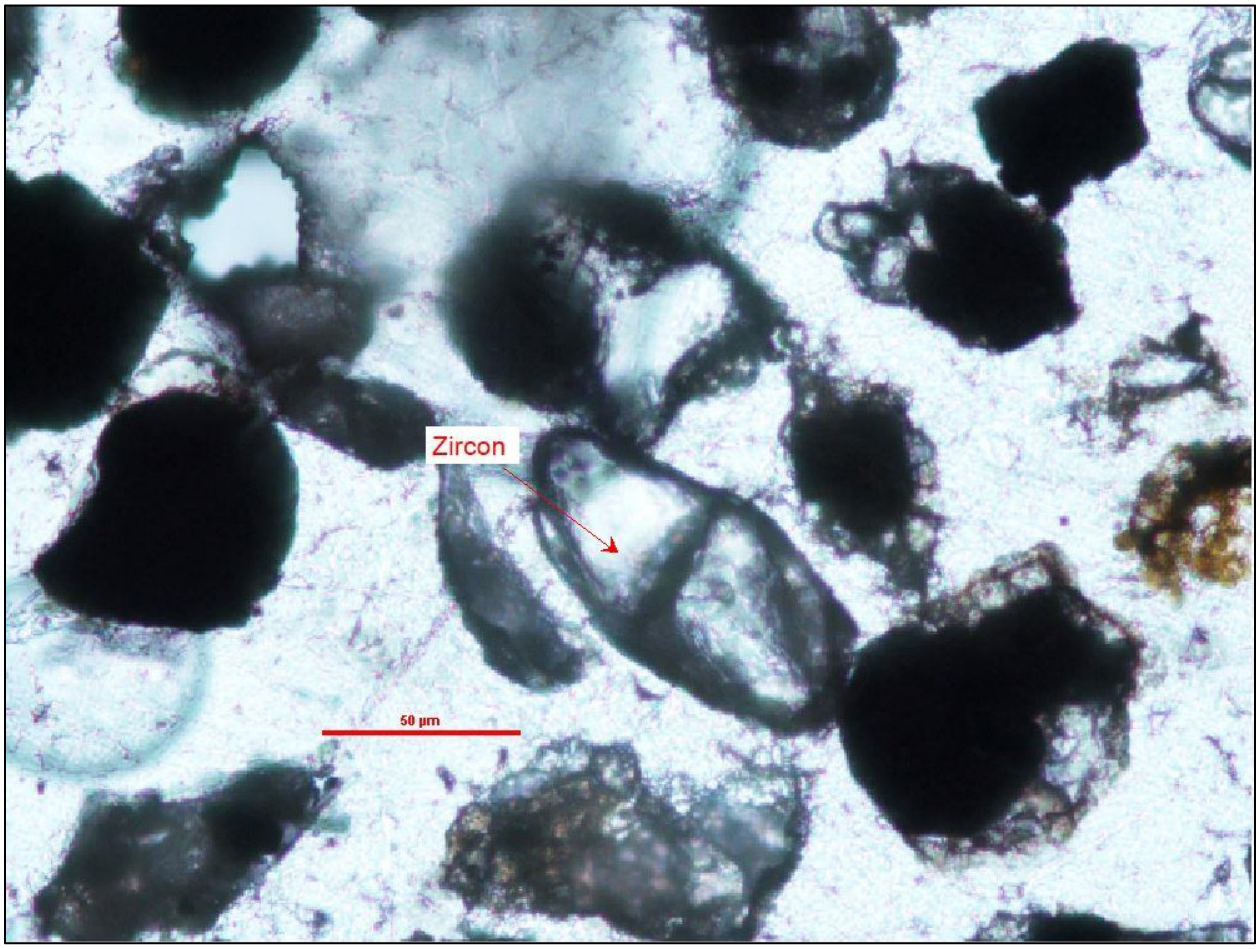

Figure 11. Photograph of sample 17IB02 showing tourmaline, fluorite, glauconite, and pyrite grains at 40x magnification. Photo by Jonathan Vitali.

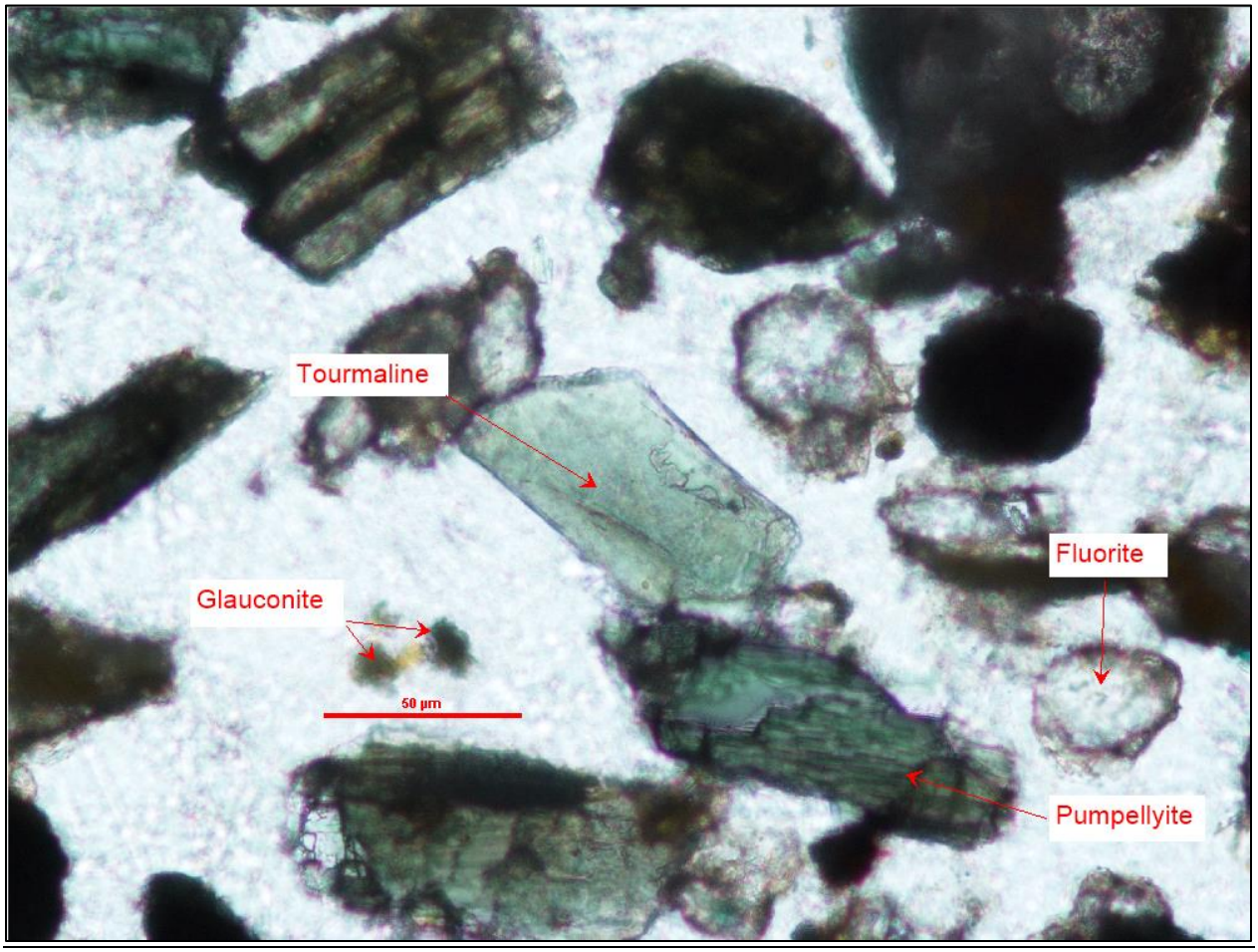

Figure 12. Photograph of sample 17IB03 showing chlorite, fluorite, glauconite, and pyrite grains at 40x magnification. Photo by Jonathan Vitali.

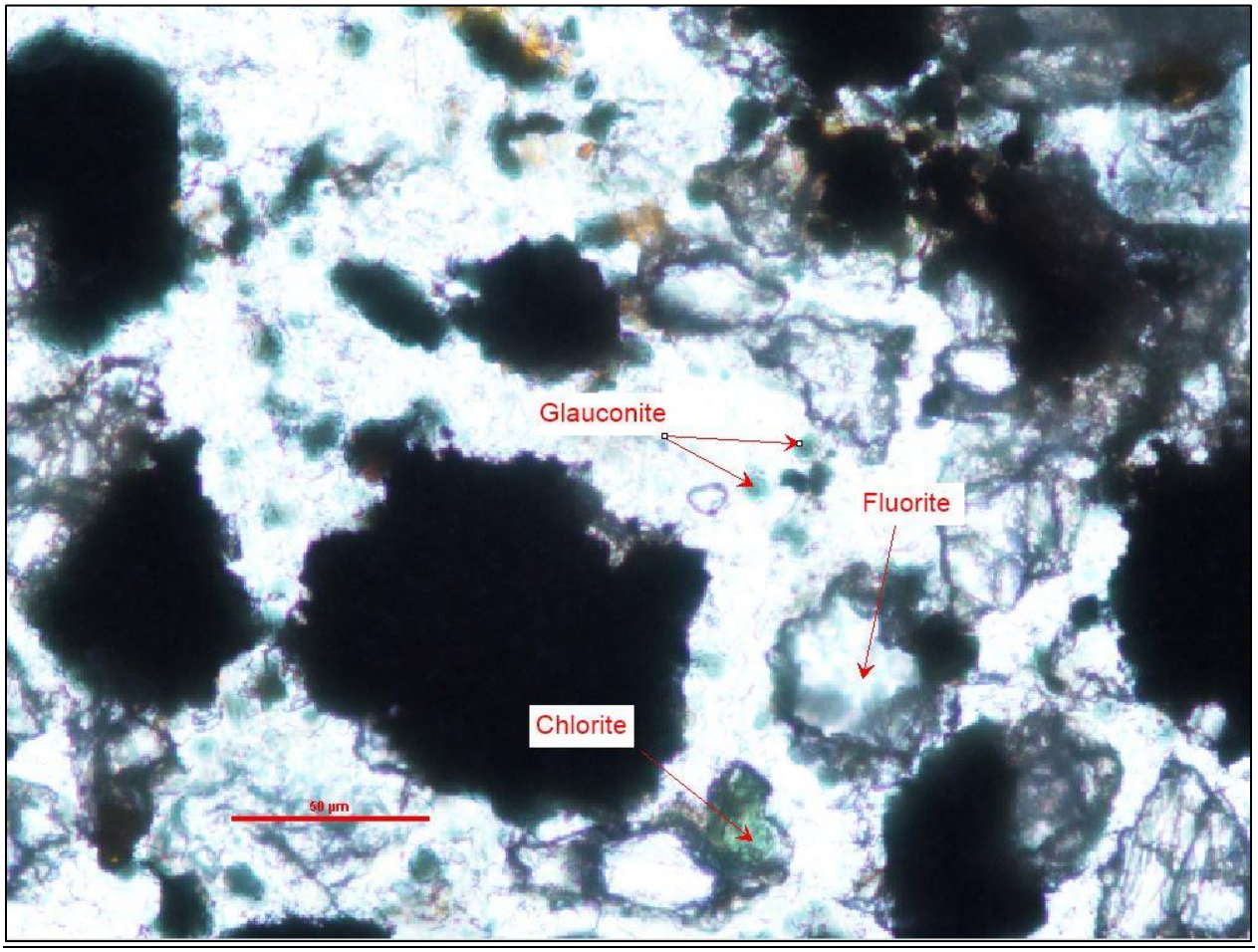

Figure 13. Photograph of sample 17IB04 showing chlorite, glauconite and pyrite grains at 40x magnification. Photo by Jonathan Vitali.

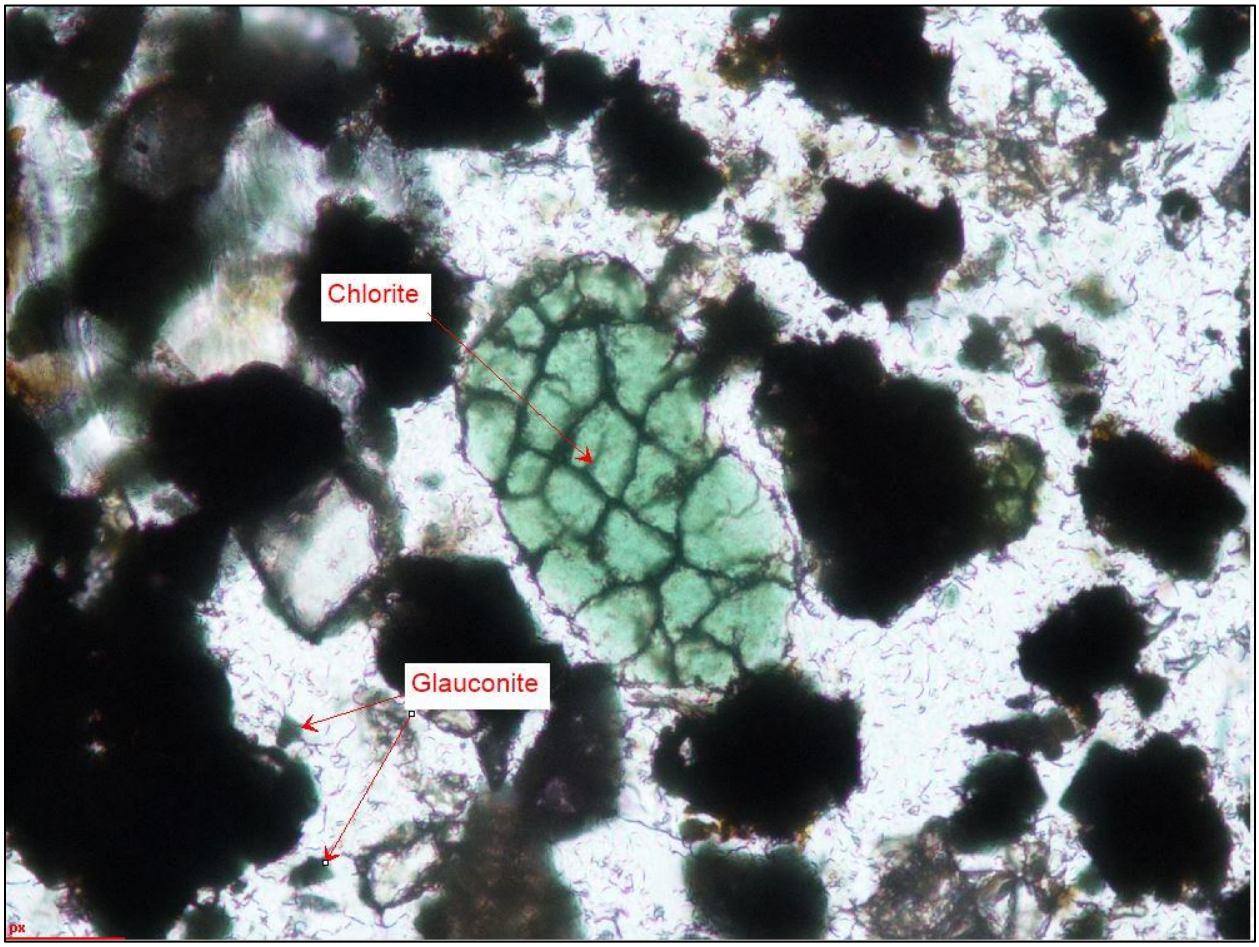

Figure 14. Photograph of sample 17IB05 showing chlorite and glauconite grains. Opaque grains are believed to be pyrite. Magnification is 40x. Photo by Jonathan Vitali.

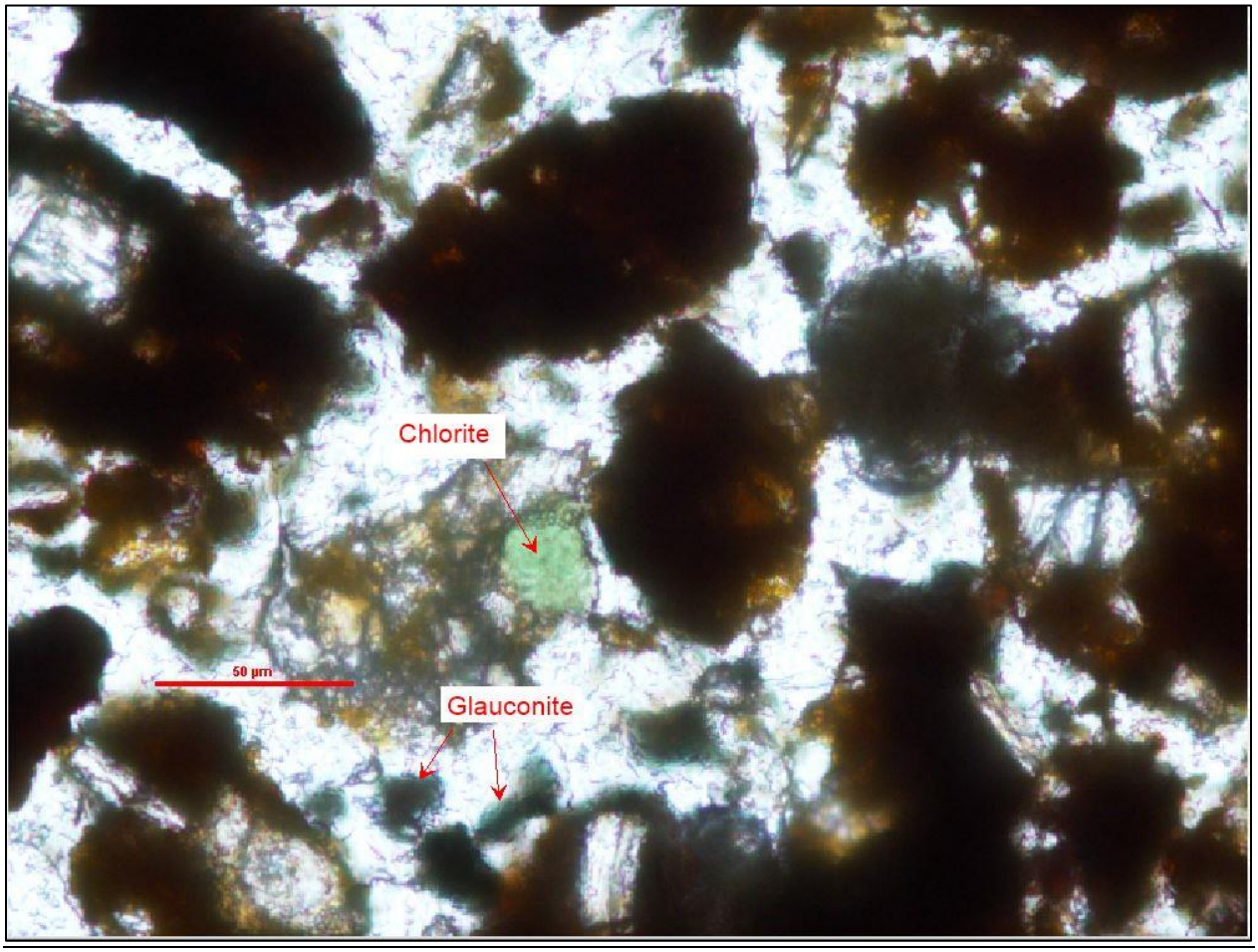

Figure 15. Photograph of sample 17IB06 showing pumpellyite and glauconite grains. Opaque grains are believed to be pyrite based on SEM data. Magnification is 40x. Photo taken by Jonathan Vitali.

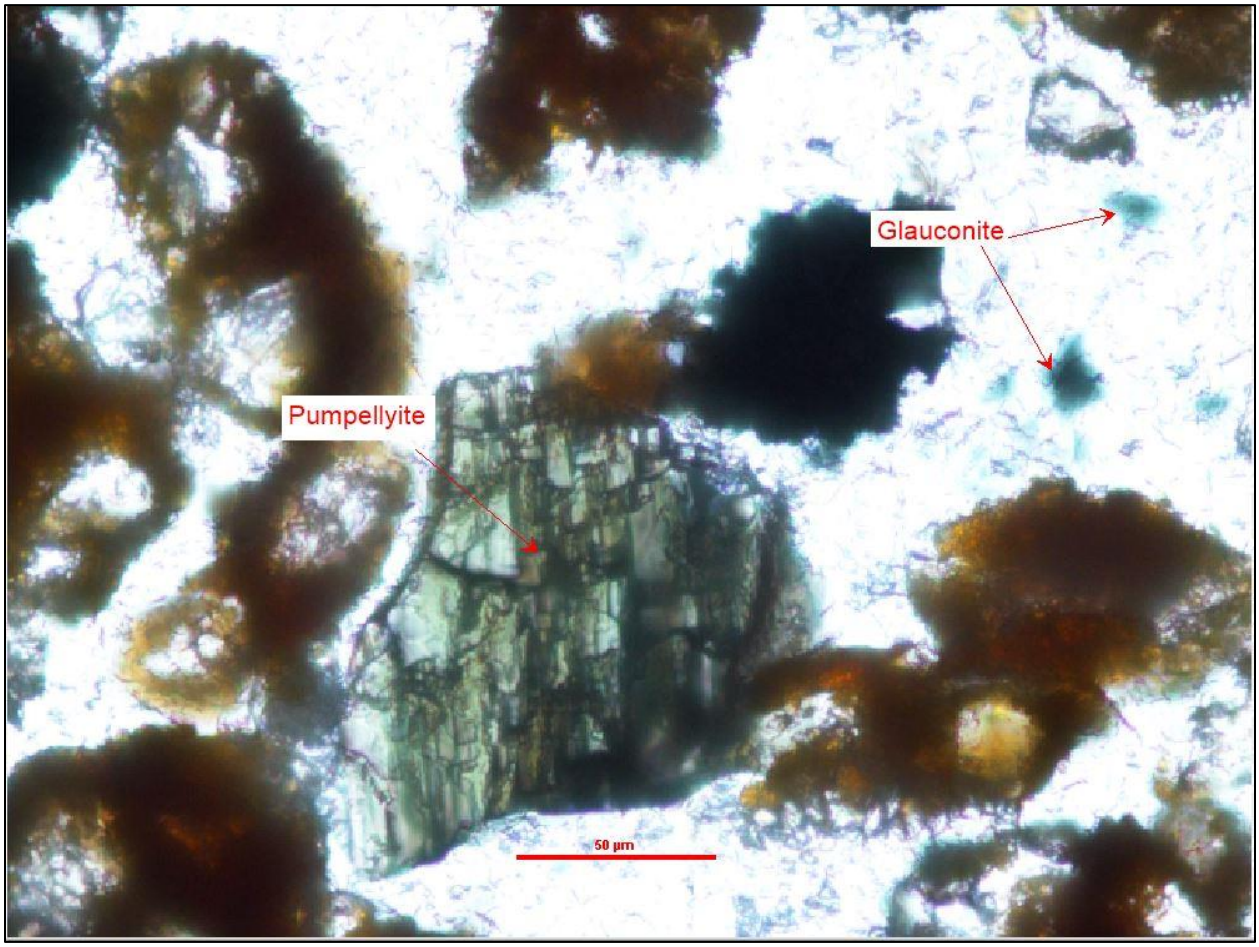

Figure 16. Photograph of sample 17IB07 showing sapphirine, rutile, and fluorite grains. Magnification is 40x. Photo by Jonathan Vitali.

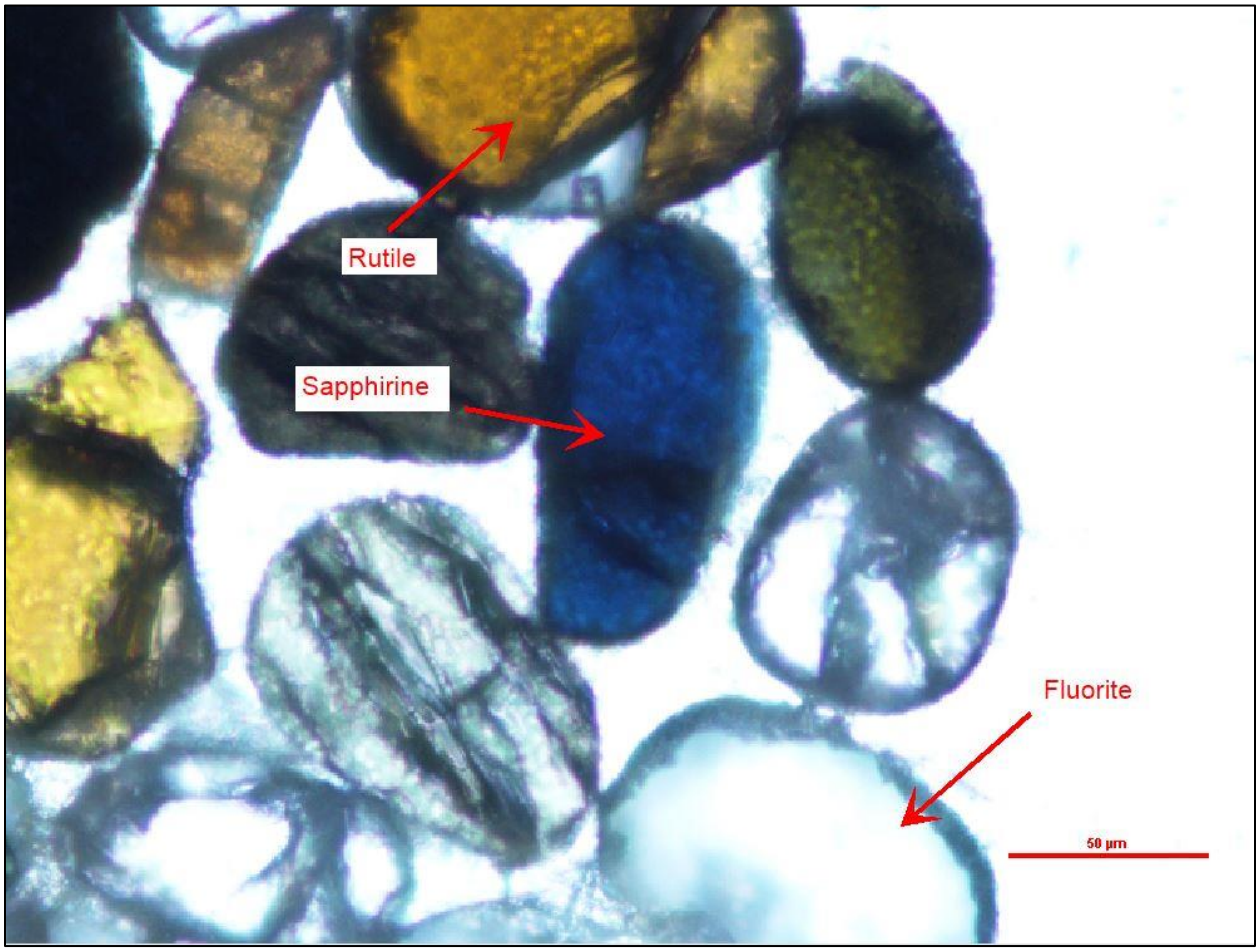

V. Discussion

Whole Rock Geochemistry

The results from XRF performed on the sample set yield important information concerning each sample's whole rock geochemistry. The standards each element is compared to are from igneous rocks, possibly leading to an amount of error that must be taken into consideration when evaluating the results. However, the weight percentages are still considered to be useful for the purposes of categorizing the whole rock samples in greater detail. Sample characteristics from hand sample and thin section descriptions (Appendix A) serve as a supplement to the XRF data.

Figure 17 is created by plotting [log (Fe_2O_3/K_2O)] against [log (SiO_2/Al_2O_3)] for each sample. The sample is then categorized by where it plots on the graph. Category boundaries are taken from Rollinson (1993). 17IB01 plots in the arkose category. This sample contains the least amount of SiO_2 at 9.4%, and highest CaO at 48.77%. However, it does not react to HCl, leading to the conclusion that the calcium is likely from Ca-feldspars, which fits the arkose classification. 17IB02 and 17IB05 plot into the shale category, yet are close to the boundary with the wacke category. However, neither of these samples exhibit the characteristic thin breaking pattern seen in shales. In this case, two conclusions can be made. The first is that these samples are actually siltstones, but plot in the shale category due to a lack of a siltstone category. Grain size analysis and the blocky form of these samples support this conclusion. The second conclusion is that these samples should plot in the wacke category, but the slight error due to using igneous XRF standards cause them to be out of position. 17IB06 also plots in the shale category. Unlike 17IB02 and 17IB05, this sample breaks into thin sheets, leading to the conclusion that it is, in fact a shale. 17IB06 is also the farthest of the three samples from the boundary with the wacke

category. 17IB03 falls within the wacke category on the graph. Its classification is supported by the sample's physical characteristics. 16IB02, 16IB01, and 17IB04 plot in the litharenite category. Lithic fragments can be observed in thin sections of all three samples. In addition, 17IB04 and 17IB05 both contain carbonate material and are over 50% matrix. Both samples also react to HCl. This leads to the conclusion that these samples are calcareous mudstones, with lithic fragments included in the rock.

Sample Provenance

Through the analytical methods mentioned earlier, an assemblage of detrital heavy minerals has been identified. For a mineral to be considered "identified", there must be at least one grain under the petrographic microscope that meets the optical characteristics of the mineral. SEM element data can be used to help identify minerals, but it cannot identify them alone. For example, cerium is reported in the bulk spectra of many of the samples, yet only one monazite grain can be identified in 16IB01. It can be inferred that there are other monazite grains throughout the sample set that are too small or obscured to identify, but not confirmed. Pumpellyite is found in abundance in sample 17IB02, and in lesser amounts in sample 17IB06. This mineral is associated with areas of low-grade metamorphism and has been found in metamorphic rocks on the west side of the Appalachian Metamorphic Belt (Zen, 1976). Chlorite is present in sample 17IB04 and is also common in low-grade metamorphic rocks, particularly greenschist. Tourmaline is found in samples 16IB01 and 17IB02, and often forms in igneous and metamorphic rocks (Figures 11and 14; Mange and Maurer, 1992). Tourmaline has also been identified throughout the Appalachians in past studies (Slack, 1982). Two forms of titanium dioxide are found in the sample set. Rutile is present in 16IB01 and 17IB07, while anatase is only identified in the latter (Figures 11 and 18). Monazite is identified only in 16IB01, and is

found in medium to high-grade metamorphic rocks (Figure 11; Mange and Maurer, 1992). Sapphirine is a rare magnesium silicate exclusive to 17IB07 and forms in high-grade metamorphic situations (Figure 18). The formation of the Appalachian mountain belt would provide the temperature and pressure required for the formation of this mineral.

Zircon is identified in seven samples, with the exceptions being 17IB06 and 17IB05 (Figure 13). The mineral's high level of resistance to weathering leads to its presence in areas as old as the Canadian Shield, were other heavy minerals break down much earlier. This means that zircon alone cannot determine if the sediments originated from the Appalachian region. The entire heavy mineral assemblage must be taken into account to determine the sediment source.

Diagenetic Processes

With the exception of sample 17IB07 from the Pendleton sandstone bed, other samples contained a high percentage of sulfides, indicative of significant diagenesis within the sampled areas of the Borden Group. Pyrite production can occur at a range of temperatures, via biotic and abiotic methods. Anaerobic sulfate-reducing bacteria facilitate the production of pyrite by catalyzing for the reaction $FeS \rightarrow FeS_2$ when sulfate is present. Laboratory tests showed both biotic and abiotic pyrite being produced at room temperature, with biotic crystals becoming larger and more plentiful than their abiotic counterparts in the same timespan (Donald and Southam, 1999). In addition to pyrite, SEM electron beam results indicate the presence of zinc sulfide (sphalerite) grains. Samples 17IB01 and 17IB04 contain the highest amounts of sphalerite within the 20-grain datasets. A possible explanation for this occurrence is the movement of zinc-rich hydrothermal fluid through the sample's location within the Borden sometime after deposition. The anatase found in 17IB07 indicates that titanium may have been a constituent in some of the fluids as well. The rectangular shape of the anatase grains indicate that they have not

experienced the same amount of weathering as the other grains found in 17IB07, and therefore may be authigenic. However, fluid inclusion analysis must be performed in order to gain a more definitive description of the hydrothermal fluids that have passed through the Borden Group and Pendleton Sandstone bed.

Fluorite grains have been identified in 5 of the samples serve as further evidence of hydrothermal fluid alteration in the study area. Another marker of diagenesis is the presence of glauconite found throughout the majority of the samples. It appears as dark green, irregularly shaped grains that tend to be much smaller than other mineral grains nearby. Since glauconite only forms in marine environments, it is determined to be authigenic in this case, as the Borden Group was deposited as a delta system and the sediment source is non-marine (Mange and Maurer, 1992). Interestingly, garnet has not been identified in any of the samples. This is unexpected, as garnets are commonly formed in high-grade metamorphism, such as mountain building. In addition, garnets are physically resistant with a hardness of 6.5-7.5 on the Mohs scale, and can withstand transportation from their source region. However, the garnets are not as stable in terms of chemical processes. Embrechts and Stoops (1982) determined that garnets are subject to dissolution processes in soils, where etches in the grains are gradually filled in with goethite, an iron oxide, over time. It is plausible that similar processes occurred in the sample locations, as iron oxides were found within the heavy mineral assemblage.

Secondary Mineralization

Several previous studies indicate the possibility for mineralization within the Borden. Shaffer (1981) investigated the possibility of Mississippi Valley-type deposits in Indiana. These deposits consist of lead-zinc ore deposits, and are common within the Illinois Basin and surrounding areas. Sphalerite and fluorite are minerals associated with these deposits. The author

stated that the sphalerite and fluorite formed when heated, metal-rich brines flowed through the rock units, causing mineralization (Shaffer, 1981).

The brines within the Illinois Basin are proposed to have originated from infiltrating surface water that became concentrated in salt via evaporation. The flow of the brines was driven by topography, where the infiltrated water flowed from higher hydraulic head on the margins if the basin towards lower head within the basin (Rowen and De Marsily, 2001). Pelch et al (2015) performed further analysis on fluid inclusions of minerals within the Illinois-Kentucky district, a Mississippi Valley-type deposit located in the southern Illinois Basin. Results indicated that mixing of sulfide-rich and sulfide-poor fluids facilitated the precipitation of sulfide minerals, which make up a majority of heavy minerals found in all samples in this project, with the exception of 17IB07. Pelch et al (2015) also estimated the time of mineralization to be late Pennsylvanian, during the Alleghanian Orogeny (Pelch et al, 2015).

Figure 17. Plot showing which category of rock each sample coincides with, based on calculations of oxide weight percentages gathered from XRF data. Category boundaries are from Rollinson (1993), figure created by Jonathan Vitali in Microsoft Excel 2013.

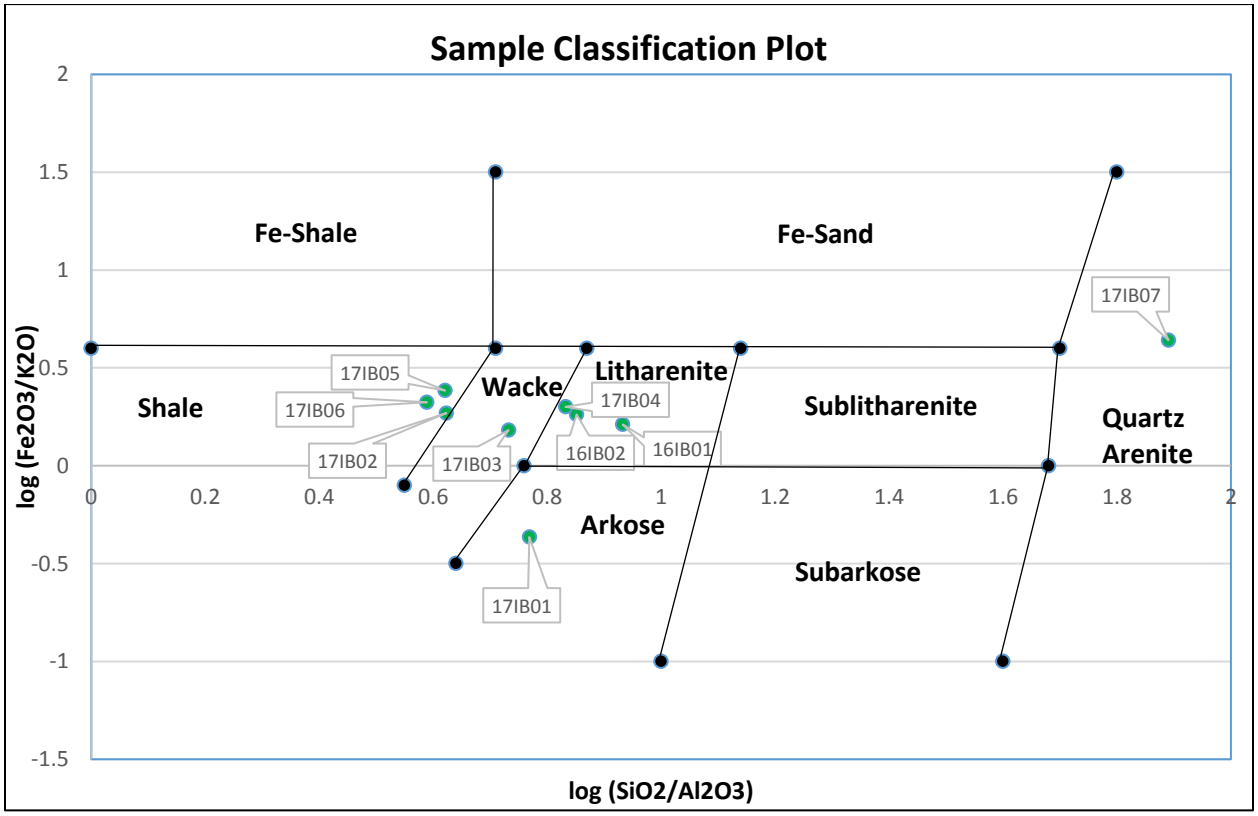

VI. Conclusions

Based on the data gathered and presented in the results section, it is determined that the main sediment source for the Borden Group is the Appalachian region. This hypothesis is supported by the variety of heavy minerals identified throughout the nine samples used in this study, by both geochemical and optical methods. It is still possible that some sediments may originate in the Canadian Shield, but they are masked by the heavy mineral suite from the Appalachian region. Further studies, such as those which utilize zircon age dating, would be required to determine the difference between zircons from the Canadian Shield and Appalachian region.

From a diagenetic perspective, the mineralogical data indicates that the Borden Group has experienced multiple forms of diagenesis. The presence of pyrite suggests an anoxic environment, a condition that would occur once the sediments were underwater and buried. The presence of glauconite is also an indicator of underwater diagenesis, as it forms only in marine environments, whereas the sediment source was a non-marine orogenic environment. The Borden Group is also determined to have experienced one or more hydrothermal fluid events. Evidence for this occurrence is found in the mineralization of sphalerite and presence of fluorite in the samples, both of which are associated with hydrothermal fluid intrusions. The anatase found in 17IB07 would also indicate hydrothermal activity if it is authigenic. Future studies can include fluid inclusion analyses in order to learn more information about the timing, source, and number of hydrothermal fluid intrusions.

References Cited

Algeo, Thomas J., et al. "Meteoric-burial diagenesis of Middle Pennsylvanian limestones in the Orogrande Basin, New Mexico: water/rock interactions and basin geothermics." *Journal of Sedimentary Research* 62.4 (1992).

Ausich, William I.et al. "Fossil communities of the Borden (Mississippian) delta in Indiana and northern Kentucky." *Journal of Paleontology* (1979): 1182-1196.

Bethke, Craig M.,et al. "Long-range petroleum migration in the Illinois Basin." *AAPG Bulletin* 75.5 (1991): 925-945.

Calhoun, J, et al. "Provenance analysis of Pennsylvanian sandstones in the Illinois Basin using detrital zircon geochronology." *Abstracts with Programs - Geological Society of America* 44 (2012) 71.

Damberger, Henz H. "Coalification pattern of the Illinois Basin." *Economic Geology* 66.3 (1971): 488-494.

Devera, Joseph A., et al. "Middle Devonian Series through Mississippian System (Kaskaskia Sequence)." Geology of Illinois, edited by Dennis R. Kolata and Cheryl Nimz, Univ. of Illinois, 2010, pp. 167–186.

Dickinson, William R., et al. "Provenance of North American Phanerozoic sandstones in relation to tectonic setting." *Geological Society of America Bulletin* 94.2 (1983): 222-235.

Donald, Ravin, and Gordon Southam. "Low temperature anaerobic bacterial diagenesis of ferrous monosulfide to pyrite." *Geochimica et Cosmochimica Acta* 63.13-14 (1999): 2019-2023.

Droste, John B., and Robert H. Shaver. "Jeffersonville Limestone (Middle Devonian) of Indiana: stratigraphy, sedimentation, and relation to Silurian reef-bearing rocks." *AAPG Bulletin* 59.3 (1975): 393-412.

Embrechts, J., and G. Stoops. "Microscopical aspects of garnet weathering in a humid tropical environment." *European Journal of Soil Science* 33.3 (1982): 535-545.

Ettensohn, Frank R. "The Catskill delta complex and the Acadian orogeny: A model." *The Catskill delta: Geological Society of America Special Paper* 201 (1985): 39-49.

Hall, Wayne E., and Irving Friedman. "Composition of fluid inclusions, Cave-in-Rock fluorite district, Illinois, and Upper Mississippi Valley zinc-lead district." *Economic Geology* 58.6 (1963): 886-911.

Hatcher, Robert D., et al. "The Appalachian orogen: A brief summary." *From Rodinia to Pangea: The Lithotectonic Record of the Appalachian Region: Geological Society of America Memoir* 206 (2010): 1-19.

Heidlauf, D. T., et al. "Tectonic Subsidence Analysis of the Illinois Basin." *The Journal of Geology* 94.6 (1986): 779-94. Web.

Houseman, Gregory, and England, Philip. "A Dynamical Model of Lithosphere Extension and Sedimentary Basin Formation." *Journal of Geophysical Research* 91.B1 (1986): 719.

Kepferle, Roy Clark. Stratigraphy, petrology, and depositional environment of the Kenwood Siltstone Member, Borden Formation (Mississippian), Kentucky and Indiana. Vol. 1007. US Govt. Print. Off., 1977.

Kissock, J.K., Finzel, E.S. 2015 "Provenance of early-middle Pennsylvanian sandstones of the Midcontinent: Detrital zircon evidence for the unroofing of Appalachian orogenies in Iowa." *Geological Society of America Abstracts with Programs* 47 (2015) 590.

Kolata, Dennis R., and W. John Nelson. "Tectonic History of the Illinois Basin: Chapter 18: Part I. Illinois Basin: Evolution." (1990): 263-285.

Konstantinou, Alexandros, et al. "Provenance of quartz arenites of the early Paleozoic midcontinent region, USA." *The Journal of Geology* 122.2 (2014): 201-216.

Leach, David L., et al. "A deposit model for Mississippi Valley-Type lead-zinc ores: Chapter A in Mineral deposit models for resource assessment." No. 2010-5070-A. US Geological Survey, 2010.

Macke, D. L., 1995, Illinois Basin Province (064), in Gautier, D. L., Dolton, G.L., Takahashi, K.I., and Varnes, K.L., ed., 1995 National assessment of United States oil and gas resources--Results, methodology, and supporting data: U.S. Geological Survey Digital Data Series DDS-30, Release 2, one CD-ROM.

Mcbride, John H., and Dennis R. Kolata. "Upper Crust beneath the Central Illinois Basin, United States." *Geological Society of America Bulletin* 111.3 (1999): 375-94.

Montanez, Isabel P. "Late diagenetic dolomitization of Lower Ordovician, upper Knox carbonates: A record of the hydrodynamic evolution of the southern Appalachian Basin." *AAPG bulletin* 78.8 (1994): 1210-1239.

Morton, Andrew C., and Claire R. Hallsworth. "Processes controlling the composition of heavy mineral assemblages in sandstones." *Sedimentary Geology* 124.1 (1999): 3-29.

Pelch, Michael A., et al. "Constraints from fluid inclusion compositions on the origin of Mississippi Valley-Type mineralization in the Illinois-Kentucky district." *Economic Geology* 110.3 (2015): 787-808.

Pfaff, Katharina, et al. "Trace and minor element variations and sulfur isotopes in crystalline and colloform ZnS: Incorporation mechanisms and implications for their genesis." *Chemical Geology* 286.3-4 (2011): 118-134.

Rollinson, Hugh R. "Using Geochemical Data: Evaluation, Presentation, Interpretation." Routledge, 1993.

Rowan, E. L., and G. De Marsily. "Infiltration of Late Palaeozoic evaporative brines in the Reelfoot rift: a possible salt source for Illinois basin formation waters and MVT mineralizing fluids." *Petroleum Geoscience* 7.3 (2001): 269-279.

Sable, Edward G. "Paleotectonic Investigations of the Mississippian System in the United States, part I: Introduction and Regional Analyses of the Mississippian System." *Paleotectonic investigations of the Mississippian System in the United States* 1010 (1979): 59.

Shaffer, Nelson R. "Possibility of Mississippi Valley-type mineral deposits in Indiana." *Indiana Department of Natural Resources, Geological Survey* (1981).

Shaver, Robert H. et al. *Compendium of Rocks Units in Indiana- A Revision*. Indiana Geological & Water Survey, 1986.

Slack, John F. "Tourmaline in Appalachian-Caledonian massive sulphide deposits and its exploration significance." *Transactions of the Institution of Mining and Metallurgy, Section B: Applied Earth Science* 91.May (1982): 81-89.

Stewart, John H. "Late Precambrian Evolution of North America: Plate Tectonics Implication." Geology 4.1 (1976): 11.

Stockdale, Paris Buell. "Lower Mississippian rocks of the east-central interior." *Geological Society of America* 22 (1939)

Swann, David Henry. "Classification of Genevievian and Chesterian (late Mississippian) rocks of Illinois." *Report of investigations no. 216* (1963).

Swezey, C.S. "Regional stratigraphy and petroleum systems of the Illinois basin, U.S.A.: U.S. Geological Survey Scientific Investigations Map 3068" (2009).

Thomas, W.A., et al.2015. "Detrital-zircon populations and Mississippian-Permian sediment dispersal pathways in eastern Laurentia." Abstracts with Programs - Geological Society of America 47 (2015) 82.

Thompson, Todd A. et. al. "Generalized Stratigraphic Column of Indiana Bedrock." *Indiana Geological and Water Survey* (2010).

Zen, E-an. "Prehnite-and pumpellyite-bearing mineral assemblages, west side of the Appalachian metamorphic belt, Pennsylvania to Newfoundland." *Journal of Petrology* 15.2 (1974): 197-242.

VII. Appendix A. Sample descriptions based off of petrography

Sample ID	Hand Sample Description	Thin Section Description	Rock Name
16IB01	Grey in color, light/dark layering, silt-sized grains, possible fossil pieces, reacts to HCl.	60% quartz, 30% calcite, 10% opaques. Roughly equigranular.	Calcareous Siltstone
16IB02	Light brown weathered face, tan fresh face, fine-grained sand-sized grains.	80% Quartz, 15% lithics, 5% Fluorite. Rust stains visible.	Fine-grained quartz arenite
17IB01	Tan in color, rust stains on weathered face, silt-sized grains.	85% Quartz, 10% Opaques, 5% Fluorite.	Siltstone
17IB02	Grey in color, silt-sized grains. Weathered face has a brownish tint to it.	90% Quartz, 10% Opaques.	Siltstone
17IB03	Grey in color, weathered face shows dark grey staining, silt-sized grains.	90% Quartz, 5% Opaques, 5%	Siltstone
17IB04	Tan in color, weathered face is dark brown in places. Contains microfossils, reacts to HCl.	60% Brownish matrix, 30% fossils, 10% lithics.	Calcareous mudstone
17IB05	Light grey fresh face, weathered face is dark grey to rusty brown. Contains microfossils, reacts to HCl. Silt-sized	90% Grey matrix, 10% calcite grains, vein-like rust colored features.	Calcareous mudstone
17IB06	Light grey in color, silt-sized grains.	95% Quartz, 5% Opaques.	Siltstone
17IB07	White in color with rust stains, very poorly cemented, fine to medium sand grains.	90% Quartz, 7% Opaques, 3% Fluorite.	Quartz arenite

Figure A-1. Representative micrograph of sample 16IB01, with Plane Polarized light (Top) and Cross-Polarized light (Bottom).

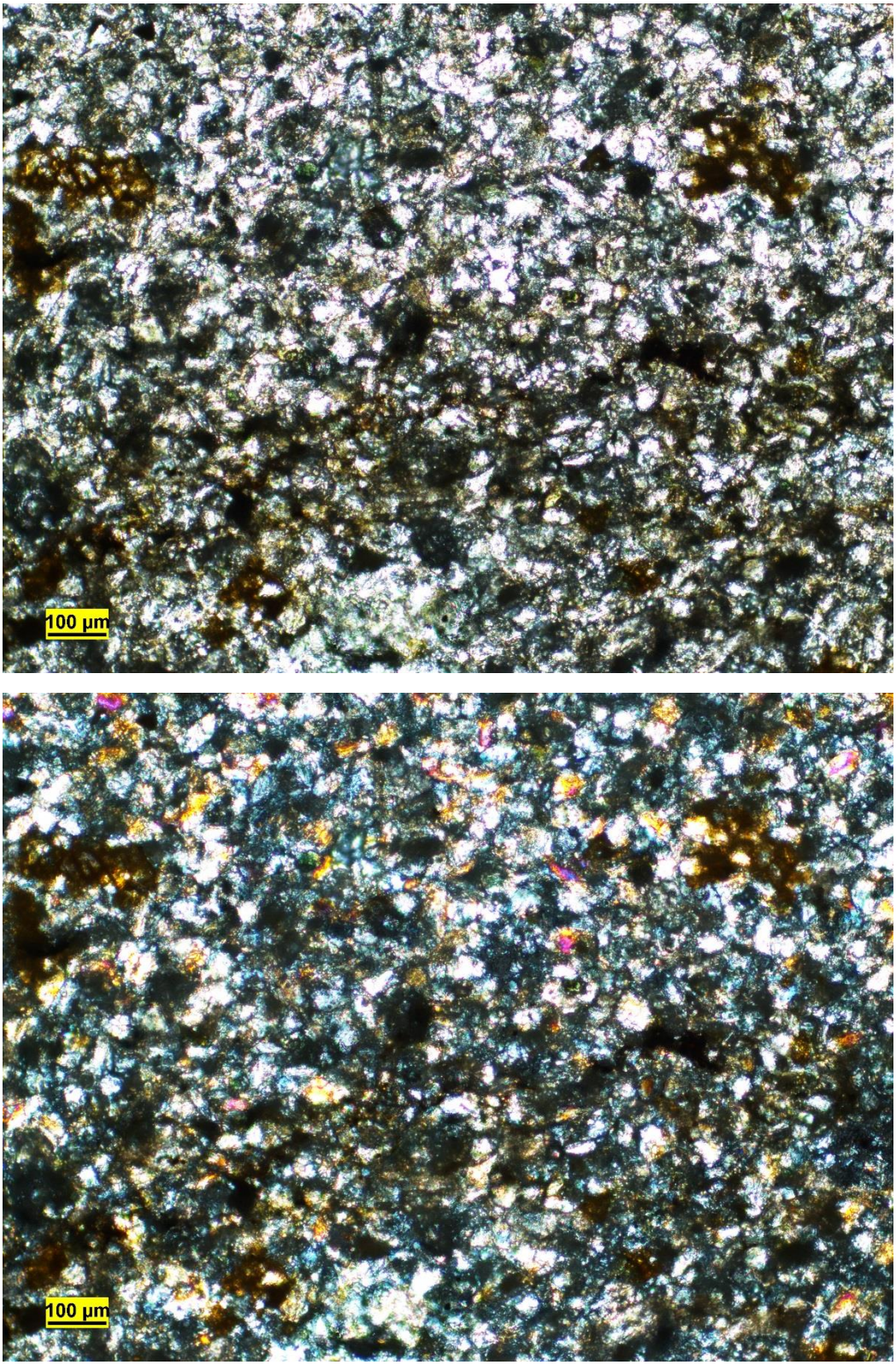

Figure A-2. Representative micrograph of sample 16IB02, with Plane Polarized light (Top) and Cross-Polarized light (Bottom).

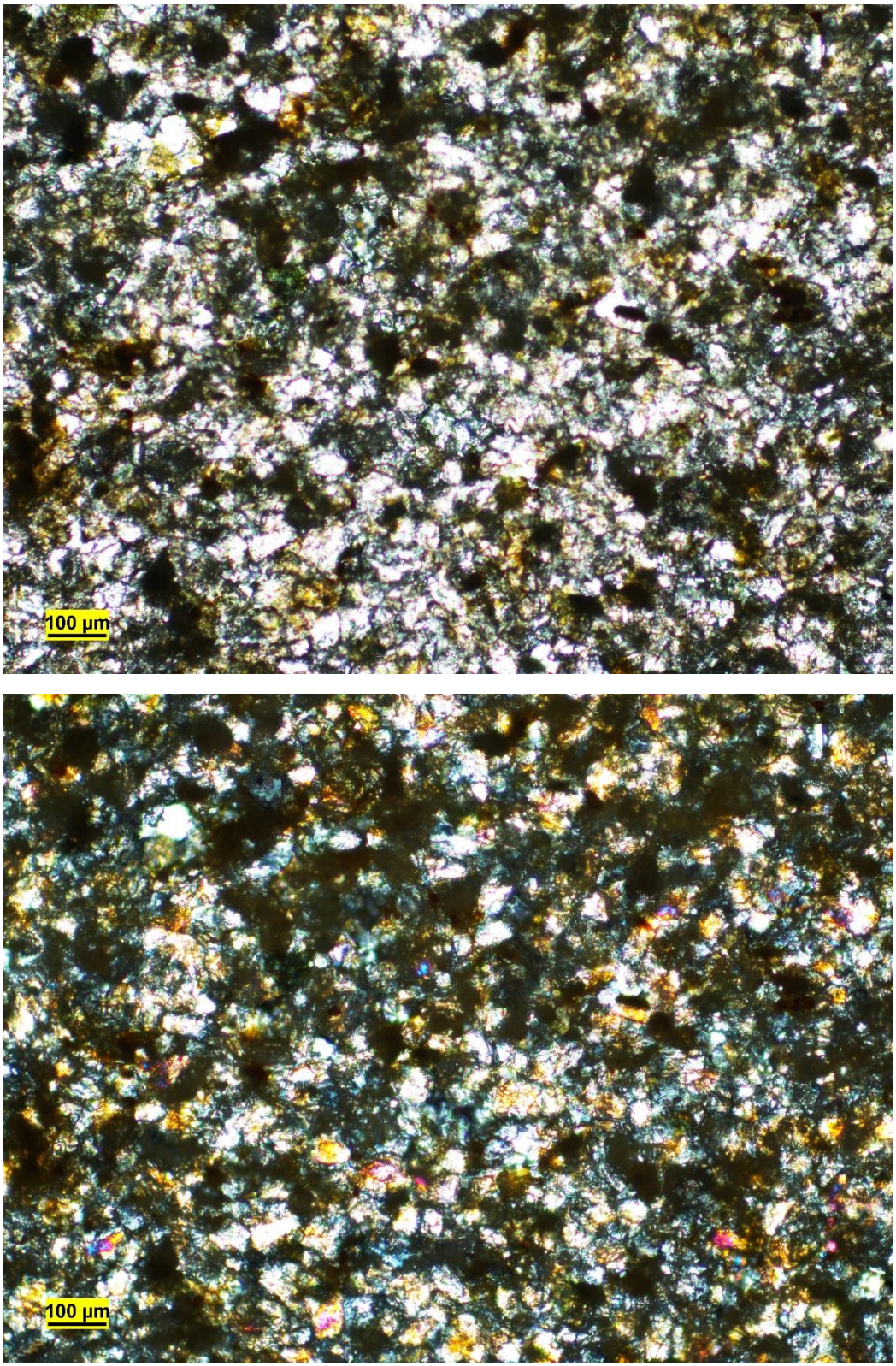

Figure A-3. Representative micrograph of sample 17IB01, with Plane Polarized light (Top) and Cross-Polarized light (Bottom).

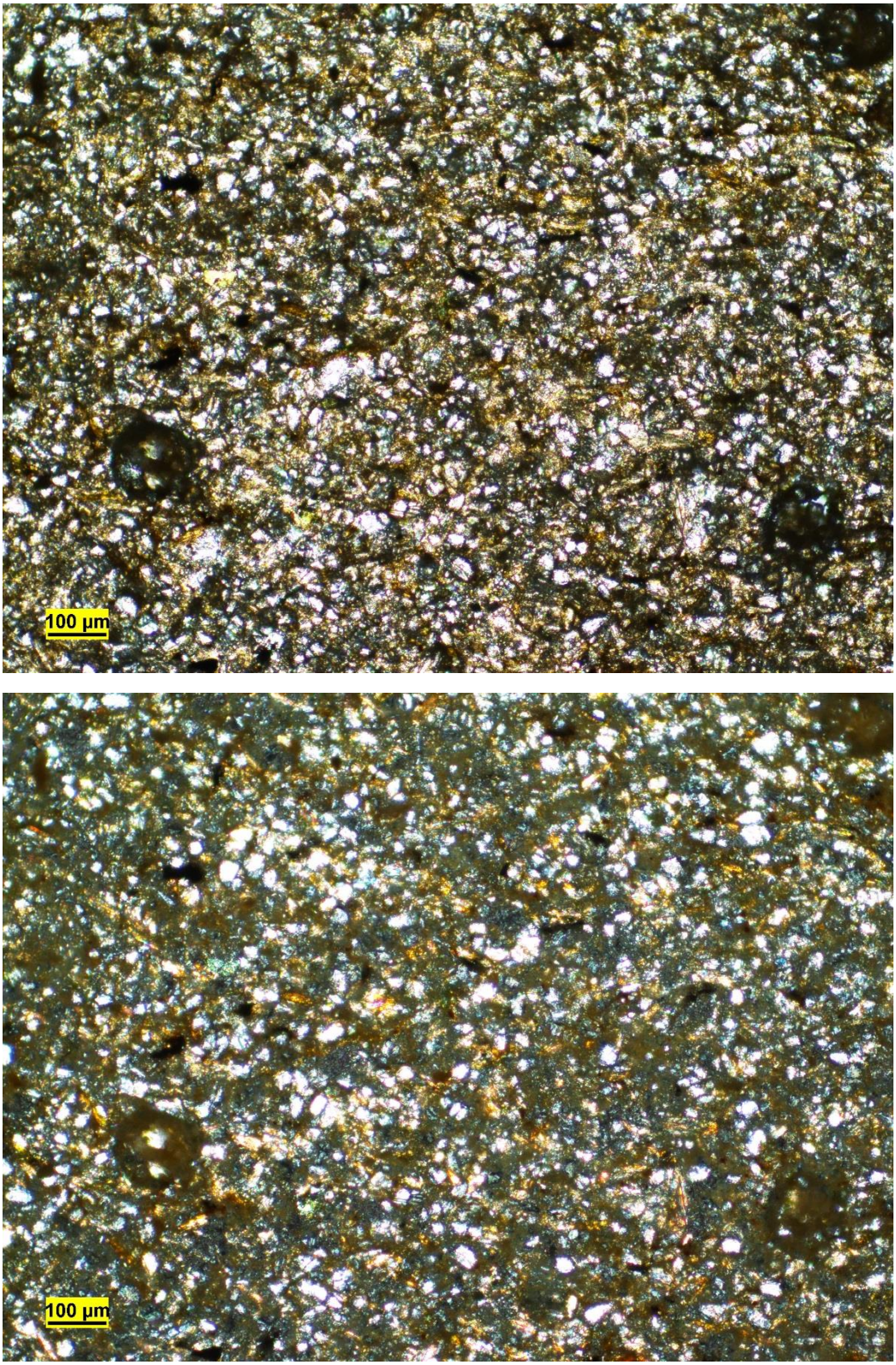

Figure A-4. Representative micrograph of sample 17IB02, with Plane Polarized light (Top) and Cross-Polarized light (Bottom).

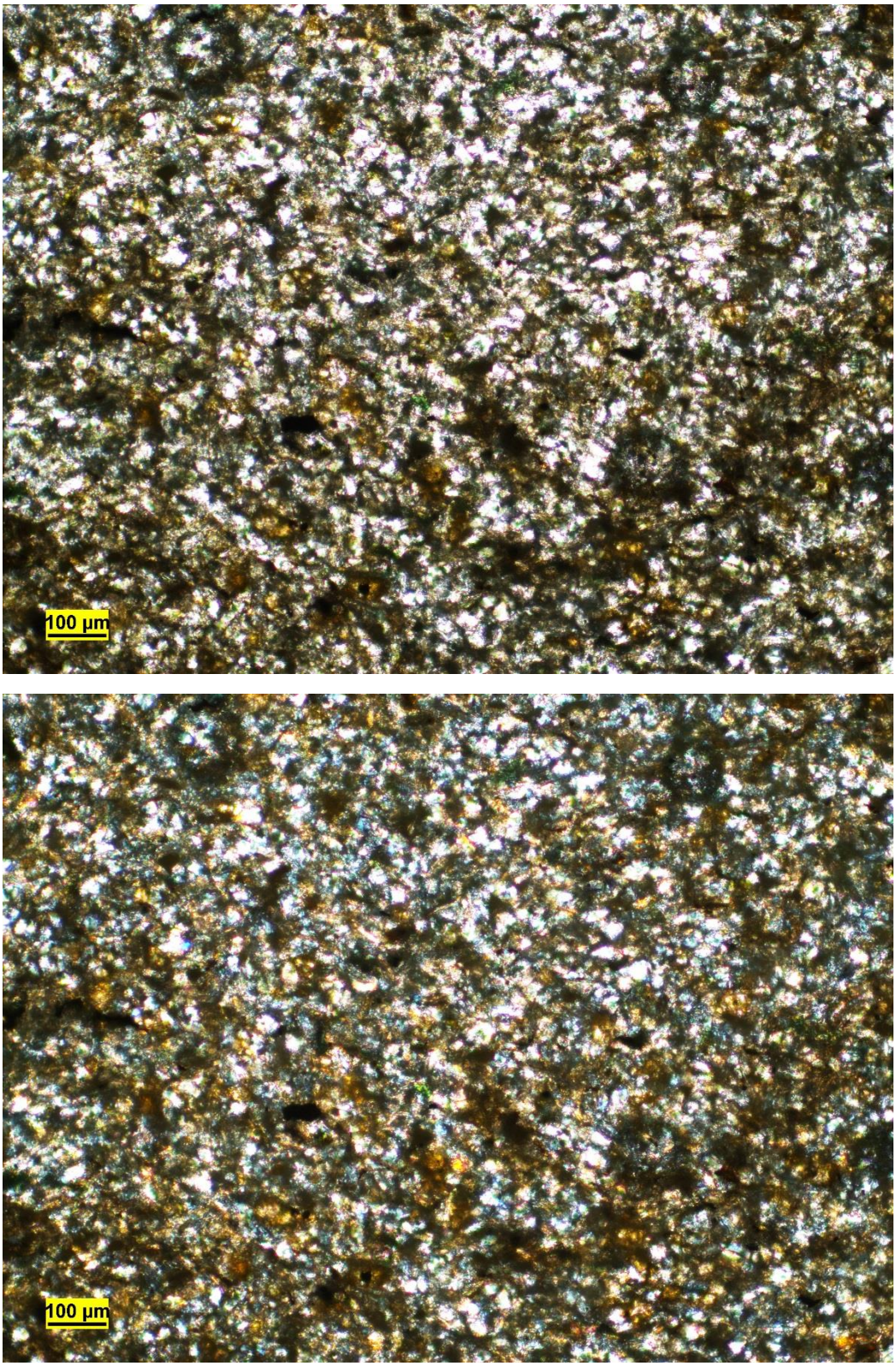

Figure A-5. Representative micrograph of sample 17IB03, with Plane Polarized light (Top) and Cross-Polarized light (Bottom).

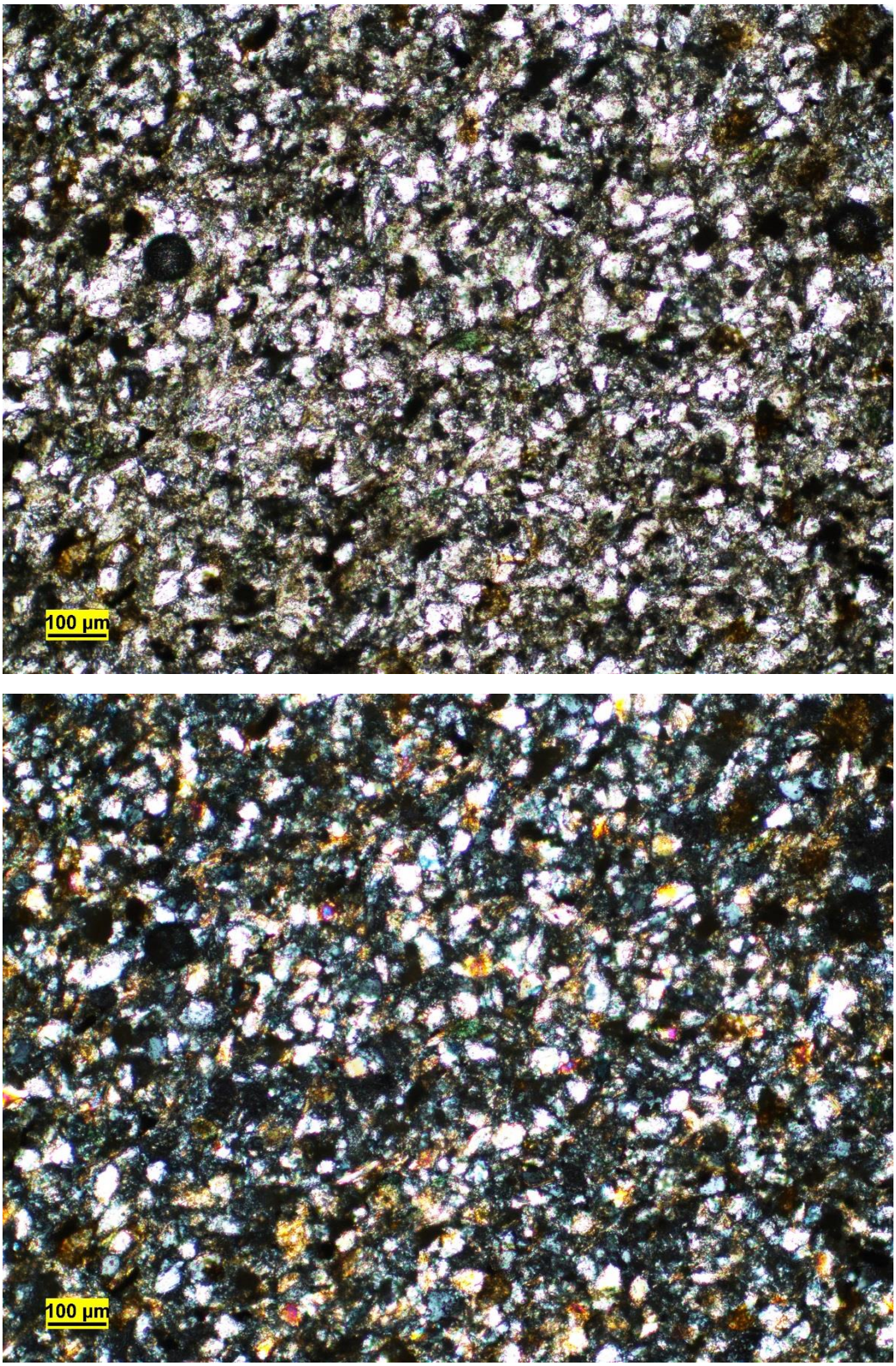

Figure A-6. Representative micrograph of sample 17IB04, with Plane Polarized light (Top) and Cross-Polarized light (Bottom).

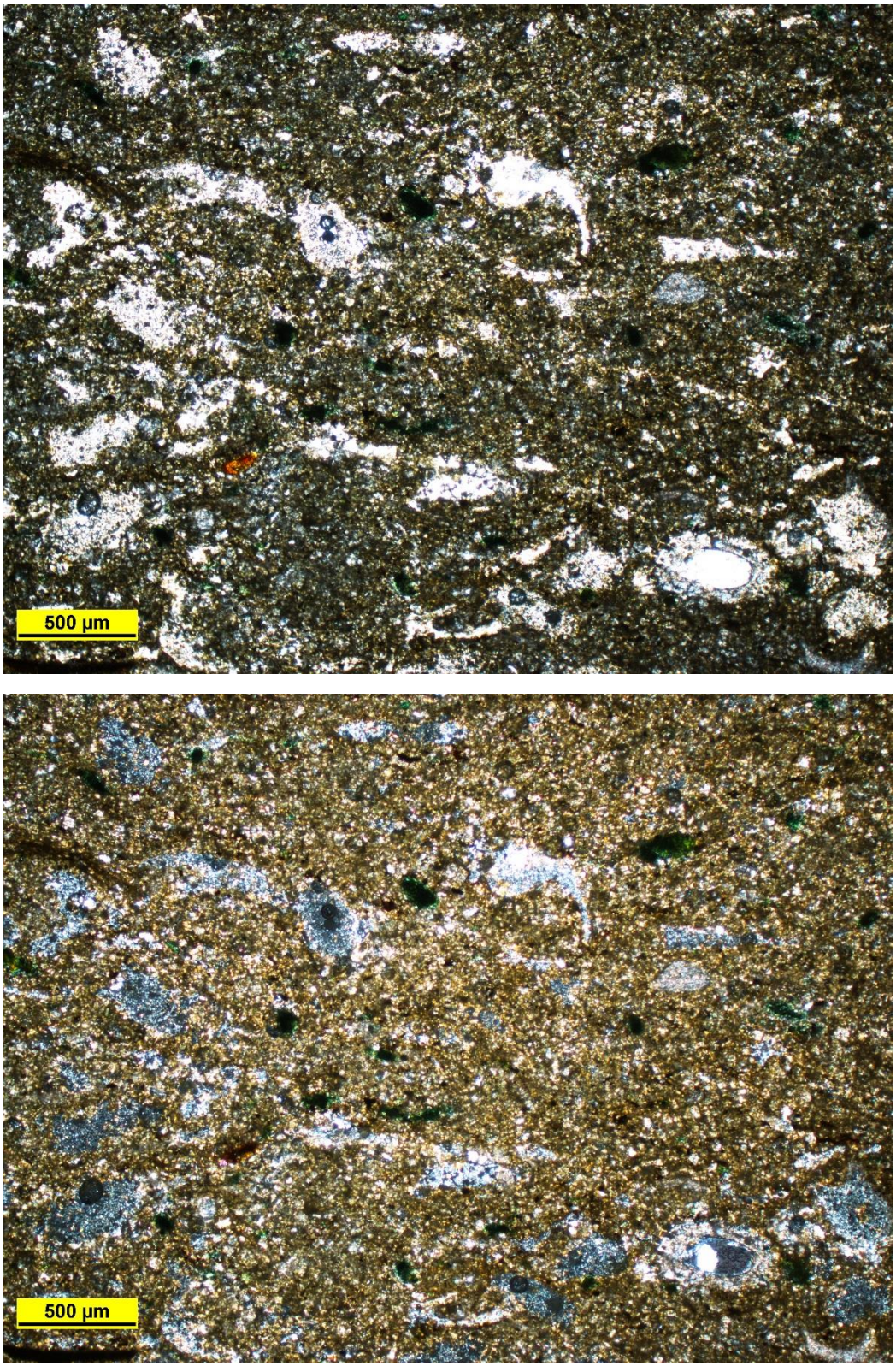

Figure A-7. Representative micrograph of sample 17IB05, with Plane Polarized light (Top) and Cross-Polarized light (Bottom).

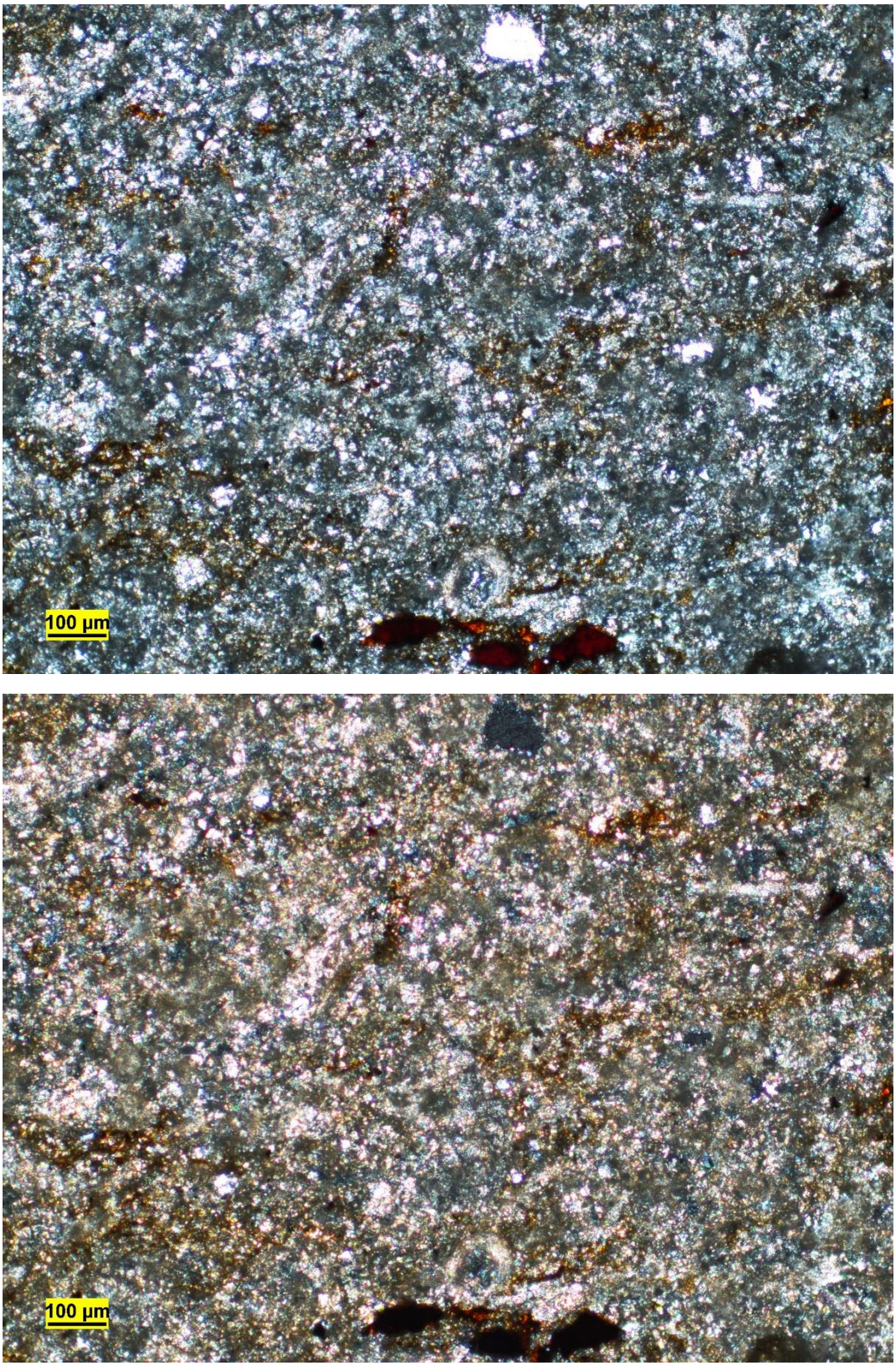

Figure A-8. Representative micrograph of sample 17IB06, with Plane Polarized light (Top) and Cross-Polarized light (Bottom).

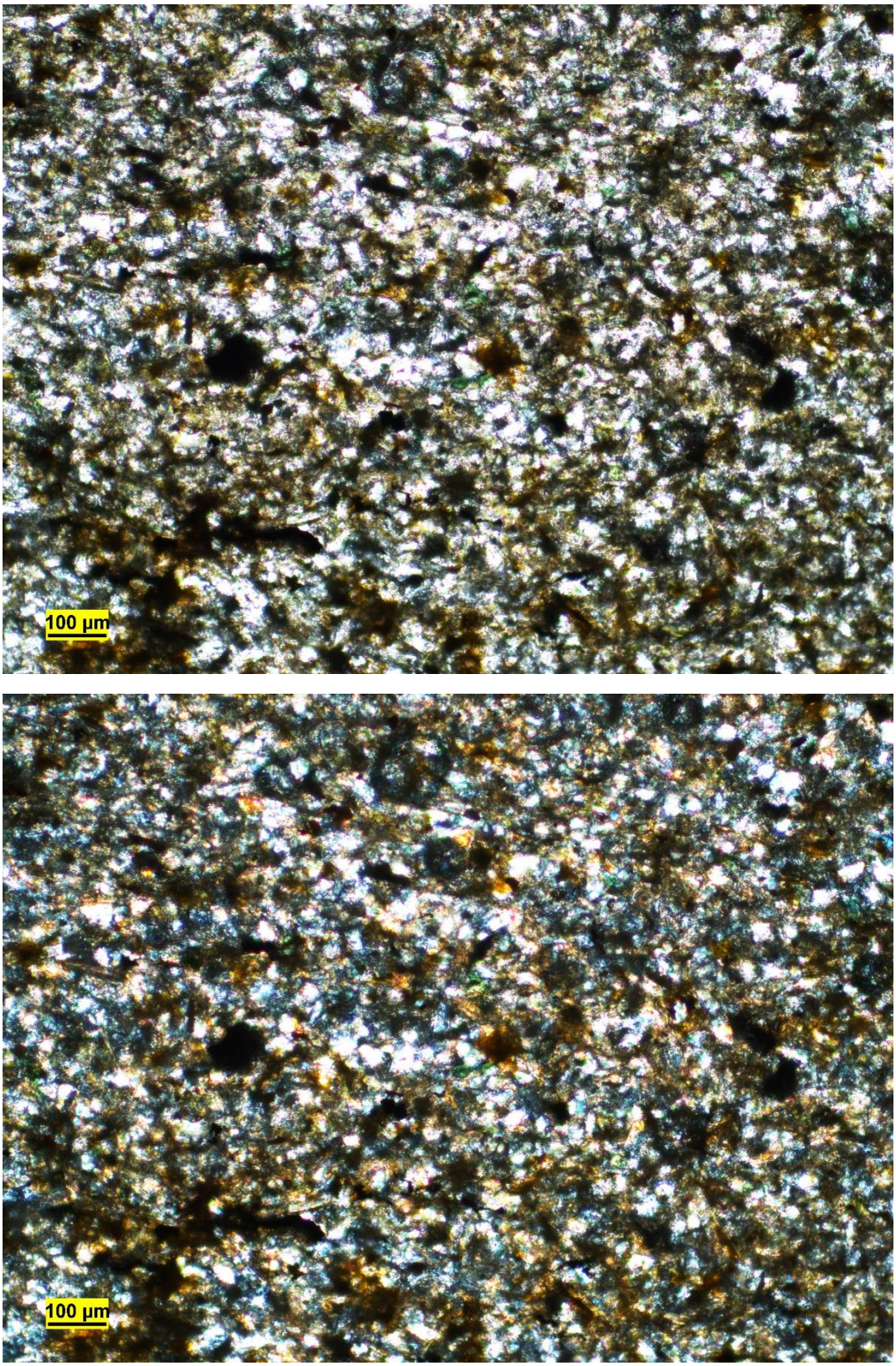

VIII. Appendix B: Grain Mount Descriptions

16IB01

- **Obs:** 75% of grains are opaque
    - Opaque grains are ***pyrite***, based on SEM data.
- **Obs:** Small, elongated hexagonal grain. Displays colorless to dark brown pleochroism, with no visible cleavages.
- Exhibits 2nd order yellow, blue, green, and pink. Colors are banded. Almost parallel extinction in xpl.
    - This grain is a ***tourmaline***.
- **Obs:** Dark green, almost opaque grains scattered throughout sample. Much smaller than other grains.
    - These are ***glauconite*** grains.
- **Obs:** elongated, colorless grain. Has a thick, black outline and high relief.
- In xpl, exhibits parallel extinction and 2nd order blue, green and yellow/orange interference colors.
    - This grain is a ***zircon***.
- **Obs:** grain #1 on SEM spectra spreadsheet located with petrographic microscope.
- Rounded, colorless, high relief. Non-pleochroic.
- Extinction is slightly off-parallel, displays 2nd order pink, yellow, blue and green.
- SEM element data indicates the presence of cerium in the grain.
    - This is a ***monazite*** grain.
- **Obs:** Grain #4 on SEM spectra sheet.
- Small, rounded grain, dark reddish brown in ppl, pleochroic, thick black rim.
- Dark brown, almost opaque in xpl. SEM data shows high amount of titanium in grain.
    - This is a ***rutile*** grain.

16IB02

- Obs: Rounded, brownish grains in ppl.
- Pleochroic, light brown to dark brown.
- Dark brown in xpl.
    - These are ***rutile*** grains.
- Obs: Colorless grains with negative relief.
    - These are ***fluorite*** grains.
- Obs: Elongated, hexagonal grain.
- Moderate relief.
- Fractures perpendicular to straight sides.
- Parallel extinction, interference colors are inhibited by fractures.
    - This is a possible ***tourmaline*** grain.
- Obs: somewhat irregular single terminated grain.
- High relief (black halo), colorless in ppl.
- Blue/green/yellow interference colors, parallel extinction in xpl.
    - This is likely a ***zircon*** grain.

17IB01

- **Obs:** 45% of grains are isotropic
- **Obs:** 50% of grains are opaque
    - Opaques are ***pyrite***, based on SEM data.
- **Obs:** isotropic grains, colorless in ppl, display negative relief
    - These are ***fluorite*** grains.
- **Obs:** colorless, elongated grain with very high relief. Exhibits parallel extinction and 2nd order pink, blue, green and yellow in xpl.
    - This is a ***zircon*** grain.
- **Obs:** Angular grains that exhibit grayish, "dusky" appearance in ppl. Isotropic.
    - These are ***sphalerite*** grains, determined in conjunction with SEM data.

17IB02

- **Obs:** 35% of grains are opaque.
    - These are ***pyrite*** grains, based on SEM data.
- **Obs:** elongated grain, high relief, black "halo" surrounding it.
- Parallel extinction, exhibits 2nd/3rd order pink, green, blue, orange/yellow. Colors appear to follow a zoning pattern.
    - This is a ***zircon*** grain.
- **Obs:** Lots of green grains under ppl. About 50% of non-opaque grains.
- Yellow green to bluish green Pleochroic.
- Fibrous nature to the grains.
    - These are ***pumpellyite*** grains.
- **Obs:** Pale green grain, lacking the fibrous nature of the pumpellyite grains.
- Pleochroic, elongated hexagonal shape, medium relief.
    - This is a ***tourmaline*** grain.
- **Obs:** colorless, subhedral grains. Isotropic with negative relief.
    - These are ***fluorite*** grains.

17IB03

- **Obs:** Grain #7 on SEM spectra table.
- Elongated shape, light tan under ppl. Medium relief.
- Near parallel extinction, 1st order whitish yellow interference colors.
- Contains Na, Al, Si, S and Fe, as per SEM element data.
    - This grain was not able to be identified.
- **Obs:** 45% of grains are opaque.
    - These are ***pyrite*** grains, based on SEM data.

- **Obs:** Grain exhibiting 2nd order blue, purple, and yellow in xpl. Colors are in a zoning pattern.
- Medium to high relief, grain is terminated at one end.
    - This is possibly a ***zircon*** grain.
- **Obs:** possible chlorite grains found throughout the sample.
- **Obs:** Lots of colorless grains in ppl that exhibit 1st order white/gray under xpl.
- Anhedral, many have fractures in them.
    - These may be quartz grains that somehow made it through the bromoform separation. Perhaps they were aggregated with heavier materials, causing them to sink.

17IB04

- **Obs:** 70% of grains are opaque.
    - These are likely ***pyrite*** mixed with some ***sphalerite*** grains, as indicated by SEM data.
- A few green grains under ppl.
- One appears to be fibrous, others appear to be scaly, like a turtle shell.
- The scaly grains appear to be almost isotropic.
    - Scaly grains are ***chlorite***, and the fibrous grain is likely to be chlorite as well. It has the same relief as the scaly grains, and chlorite can be fibrous in some cases.
- **Obs:** Three ***zircon*** grains confirmed in this sample.
- **Obs:** Colorless grains that show negative relief and isotropy.
    - These are ***fluorite*** grains.
- **Obs:** Colorless, fractured grains that exhibit first order white/grey interference colors.
    - These could be quartz, brought into the sample in a similar fashion to those found in 17IB03.
- **Obs:** Small, green "dots" throughout the sample. Very dark green, almost opaque.
    - These are ***glauconite*** grains.

17IB05

- **Obs:** 85% of grains are dark brown to black in color, almost opaque.
- **Obs:** small green grain found under ppl.
- Dark grey/ blue birefringence, no visible structures in grain.
    - This is likely a ***chlorite*** grain.

17IB06

- **Obs:** 50% of grains are dark brown, angular, non pleochroic and isotropic.
- Some of these grains appear to have inclusions that go extinct and show first order white/yellow interference colors.
    - The inclusions could be quartz grains held together by hematite, which caused them to sink in the bromoform.
- **Obs:** some colorless grains with negative relief.

    - These are ***fluorite*** grains.
- **Obs:** green grain with a radiating fibrous nature.
    - This is a ***pumpellyite*** grain.
- **Obs:** green grain with no fibers, turns a dark bluish color under xpl.
    - This is a ***chlorite*** grain.

17IB07

- **Obs:** most grains are well-rounded in this sample.
- **Obs:** abundant ***zircon*** and ***rutile*** grains.
- **Obs:** Less than 5% of the grains are opaque.
- **Obs:** colorless grains, rounded, show negative relief.
    - These are ***fluorite*** grains.
- **Obs:** Oval-shaped blue grains present throughout the sample.
- No discernible pleochroism
- Very dark blue to black in xpl, almost isotropic.
- Lacks cleavage
    - These are ***sapphrine*** grains.
- **Obs:** Grain #18 on spectra table.
- Rectangular, very high relief, black outline.
- Appears to be isotropic.
- SEM data shows 75% Ti, 18% Si, 7% Al.
    - This could be an ***anatase*** grain. The sharp rectangular shape may indicate that it is authigenic, as it should be rounded like the rest of the grains if it is the same age.

IX. Appendix C. SEM – EDS data tables from grain mount analyses

All elements (normalized)
[wt %]

16IB01	Mg	Al	Si	P	S	Cl	K	Ca	Ti	Cr	Mn	Fe	Zn	Zr	Ce	Mineral
Grain 1			8.1	10.7	11.9	6.2						33.3			29.8	monazite
Grain 2			7		26.8	23.1			17.3			25.9				ilmenite
Grain 3					56.2			4.8				39.1				pyrite
Grain 4									100							rutile
Grain 5					83.4							16.6				pyrite
Grain 6					91							9				pyrite
Grain 7			6.8		52.5							40.7				pyrite
Grain 8			16.1		33.6	11.1						39.2				pyrite
Grain 9			9.6		20.3	13.4						56.7				pyrite
Grain 10					75.3			3.7				21				pyrite
Grain 11			13.8		15.4	9.7			12.8			48.3				rutile(?)
Grain 12			2.7		74.7							22.5				pyrite
Grain 13			2.6		84.6							12.8				pyrite
Grain 14			21.2			4.1						11.3		63.4		zircon
Grain 15			33		14.6				15.9			36.5				rutile(?)
Grain 16			3.8		84.3							11.9				pyrite
Grain 17			26		45.8							28.2				pyrite
Grain 18			25.7		36.4							37.9				pyrite
Grain 19			25.6		18.2							56.1				pyrite
Grain 20			13.7		58.4	6.4						21.4				pyrite
Bulk spectrum 1	0.3	0.6	9.4	0.8	23.5	9.3	2.4	0	5.5	0.1	0	42.3	2.3	0.6	3	
Bulk spectrum 2	0.4	0.9	10.1	0	27	5.1	1.6	1	5.8	0	1.1	39.5	1.8	2.6	3	
Bulk spectrum 3	0	2	12.8	0.9	25	7	2.2	1.5	4.3	0	0	35.2	3	2.6	3.5	
Bulk spectrum 4	1	1.2	11.4	0	28.9	6.4	1.1	1.6	3.8	0	1.3	34.5	2.6	6.2	0	

All elements normalized) [wt %]

16IB02	Na	Mg	Al	Si	P	S	Cl	K	Ca	Ti	Cr	Mn	Fe	Zn	Zr	Ce
Bulk spectrum 1		0.8	3.5	45	0	2.3	6.8	0.1	0.7	16.5	0.5	0.1	0.4	0.6	22.6	0.2
Bulk spectrum 2		1.1	3.4	49.2	0	0	5.7	1.9	0	20	0	0	2.9	0.9	13.7	1.4
Bulk spectrum 3		0.1	4	46.5	0.3	0.6	6.6	2.2	1.1	22.2	0	1	2.7	1.9	10.9	0
Bulk spectrum 4		0	3.2	56.5	1.2	1.2	7.2	2.3	0.4	18.4	0.3	0	1.4	0.8	6.5	0.6
grain 1				35.6			37.7			26.7						
grain 2				25.6			4.4			4.4					65.6	
grain 3	8.9		14.9	63.4			7			5.8						
grain 4				25.8			4.6			4.3					65.2	
grain 5				87.3			5.4			7.3						
grain 6			1.3	24.5			4			5.1					65.1	
grain 7	8.7		14.7	64.5			4.5			7.7						
grain 8				86.7			5.2			8.1						
grain 9				38.3			15.2			46.5						
grain 10				24.3			3			4.8					67.9	
grain 11				26.7			4.1			4.6					64.6	
grain 12				25.6			5.9			4.6					63.9	
grain 13				88.7			4.5			6.8						
grain 14			1.7	24.3			3.5			3.4					67	
grain 15				79.1			10.6			10.4						
grain 16				23.9			2.3			4.1					69.7	
grain 17				28.8			3.2			5.7					62.3	
grain 18				35.4			8.5	5.4		50.8						
grain 19				84.8			7.2			8						
grain 20				23.8			6								70.2	

17IB01	All elements normalized) [wt %] Na	Mg	Al	Si	P	S	Cl	K	Ca	Ti	Cr	Mn	Fe	Zn	Zr	Ce	Mineral
Bulk spectrum 1		0.2	1.1	17	0	24.1	12.4	2.1	3.5	0.2	0.5	0.5	26.8	8	3.6	0	
Bulk spectrum 2		0.5	2	14.8	0.6	27.9	9.5	3.7	2.4	0.6	0.1	0	24.8	11.1	2	0	
Bulk spectrum 3	3.1	1.8	2.1	16.7	1.7	27.5	6.8	0	2.3	1.7	1.5	0.7	25.3	8	0.7	0.1	
Bulk spectrum 4		0.2	1.4	16.4	0.5	35.2	9.6	2.5	3.5	0	0	0	19.1	8.1	3.4	0	
grain 1				6.7		93.3											pyrite
grain 2				3.7		96.3											pyrite
grain 3				5.7		43.7								50.7			sphalerite
grain 4				25											75		zircon
grain 5				5.3		42.2	5.6							47			sphalerite
grain 6				3.8		83.3							12.9				pyrite
grain 7				5.7		77.9							16.4				pyrite
grain 8				6.3		65.9	8.2						15.9	3.7			sphalerite/pyrite
grain 9				2		38.2							5.5	54.3			sphalerite
grain 10				2.9		40.5								56.6			sphalerite
grain 11						42.9								57.1			sphalerite
grain 12				6.3		43.7								49.9			sphalerite
grain 13				10		35.8	11.4						42.9				pyrite
grain 14				3.9		42.2								53.8			sphalerite
grain 15						36.3							4.1	59.6			sphalerite
grain 16				4		96											pyrite
grain 17				2.1		69							28.9				pyrite
grain 18				3.7		39.9								56.5			sphalerite
grain 19				4.1		36.5								59.4			sphalerite
grain 20			20.8	23.1		29.4	26.8										Al2SiO5 mineral (?)

17IB02	All elements (normalized) [wt %] Mg	Al	Si	P	S	Cl	K	Ca	Ti	Cr	Mn	Fe	Zn	Br	Zr	Ce	Mineral
Bulk spectrum 1	0.3	5.9	31.8	0	5.3	13.2	4.2	6.7	3.1	0.6	1.4	24.4	2.4		0.6	0	
Bulk spectrum 2	0.4	3.4	31.8	2.6	6.9	12.5	4	6.6	5.7	0.3	0.1	24.2	0		0	1.4	
Bulk spectrum 3	0.1	4.8	33.7	0	6.6	8.6	4.3	6.7	3.7	0	0	26.5	0.9		4.2	0	
Bulk spectrum 4	2.6	6.7	37.2	0.1	7.3	8	3.7	5.6	3	0.6	0	20.8	3.6		0.2	0.7	
grain 1 [wt %]	6.4	13.4	51.3			6.1		22.8									pumpellyite
grain 2	9.4	12.7	57.1			5.6		15.3									pumpellyite
grain 3		8.8	58.8					32.4									pumpellyite
grain 4	8.4	14.5	60.6			8.7		7.8									pumpellyite
grain 5	9.3	15	59.9				4.1	11.7									pumpellyite
grain 6	12.6	7.7	70.8					9									pumpellyite
grain 7	10.1	19.4	70.6														pumpellyite
grain 8	10.8	18	71.3														pumpellyite
grain 9		10.4	49.8			10						29.8					pumpellyite
grain 10		10.3	47									42.7					pumpellyite
grain 11		7.5	16.3		54.9							21.3					pyrite (?)
grain 12		16.7	83.3														aluminosilicate
grain 13	8.3	12.4	42.7			9	5.6					22.1					biotite (?)
grain 14			19.5		80.5												pyrite
grain 15			28.7												71.3		zircon
grain 16	9.2	14.7	66.1			10.1											pumpellyite
grain 17			81.7			18.3											quartz
grain 18	8	0.6	50.9			18.8								21.7			garnet (?)
grain 19	13.8		69.9			16.2											pumpellyite
grain 20		14.9	60.6			14.3		10.1									pumpellyite

All elements (normalized)
[wt %]

17IB03	Na	Mg	Al	Si	P	S	Cl	K	Ca	Ti	Cr	Mn	Fe	Zn	Br	Zr	Ce	mineral
Grain 1				1.2		65.4							33.4					pyrite
Grain 2				93.2			6.8											quartz
Grain 3				93.7			6.3											quartz
Grain 4				7.2		92.8												pyrite
Grain 5				93.1			6.9											quartz
Grain 6				5.2		83.3							11.5					pyrite
Grain 7	7.3		14	51.7		6.5							20.5					unknown
Grain 8				73.5		8.8							17.7					pyrite
Grain 9				9.7		75.6							14.7					pyrite
Grain 10				4.1		83.9							12					pyrite
Grain 11				5.1		76.3							18.6					pyrite
Grain 12				71		7.7							21.3					pyrite
Grain 13				6.3		72.7							21					pyrite
Grain 14				7		78							15					pyrite
Grain 15	10.9			38.3		11.3							20.1		19.3			unknown
Grain 16				19.6		26.3	10.1						43.9					pyrite
Grain 17				22.7		19.2	8.9						49.2					pyrite
Grain 18				5		79.8							15.2					pyrite
Grain 19				18.6		21.9	12.9						46.6					pyrite
Grain 20				72.9		8.4	5.6						13.1					pyrite
Bulk spectrum 1		0	1	29.7	1.2	25.2	12.5	4.2	0	0	0	0	22.6	2.8		0.9	0	
Bulk spectrum 2		1.6	2.6	27.6	0	26.5	8.5	2.2	1.1	0	0.8	0	24.1	2.2		2.9	0	
Bulk spectrum 3		0.1	3.9	27	0	24.7	5.9	2.9	0.6	1.2	0	0	25.9	3.5		4.4	0	
Bulk spectrum 4		0	1.3	29.8	0	28.8	8.5	3	3.3	0	1.2	0	20.7	0		3.5	0	

17IB04	All elements (normalized) [wt %] Mg	Al	Si	P	S	Cl	K	Ca	Ti	Cr	Mn	Fe	Zn	Zr	Ce	Ta	Mineral
Bulk spectrum 2	0.1	1.3	11.7	0	26.2	7	2.1	0	1.3	1	1.5	37.5	6.7	3.1	0.7		
Bulk spectrum 1	0.1	1.5	13.1	0.6	27.4	7.8	2.4	1.1	0.6	0	0	33.9	7.9	3.3	0.4		
Bulk spectrum 3	0	1.6	14.9	0	33.3	6.5	0.9	1.8	0.5	0	0	33.9	2.8	2.9	0.9		
Bulk spectrum 4	0	0.9	16.2	0	33.4	6.1	1.6	0	0	0.2	0	30.3	7.5	3.8	0		
grain 1			2		47.6								50.4				sphalerite
grain 2					79.9							12				8.1	pyrite
grain 3			7.6		70							22.4					pyrite
grain 4			77.4		6							16.6					pyrite
grain 5			14.8		49	8.9						27.4					pyrite
grain 6			5		62.9	6.4	3					22.7					pyrite
grain 7			7.4		64.4							28.2					pyrite
grain 8			7.1		75.9							17					pyrite
grain 9			9.4		33	11						46.5					pyrite
grain 10			3.8		75.2							21					pyrite
grain 11			3.8		68.8							27.3					pyrite
grain 12			2.4		67.6							29.9					pyrite
grain 13			11.4		54.1							34.4					pyrite
grain 14			9.9		52.3	9.5						28.4					pyrite
grain 15			12.2		36.4	6.8						44.6					pyrite
grain 16			14.9		22.1							63					pyrite
grain 17			8.1		58.1							33.8					pyrite
grain 18			10.1		31.2							14.9	43.8				sphalerite
grain 19			13.6		38.3							48.2					pyrite
grain 20			7.3		32.3							20.9	39.5				sphalerite

17IB05	All elements (normalized) [wt %] Mg	Al	Si	P	S	Cl	K	Ca	Ti	Cr	Mn	Fe	Zn	Br	Zr	Ce	mineral
Bulk spectrum 1	0.5	7.7	18.3	0.2	2.5	5.2	2.9	1.8	0	0.2	0.8	56.6	0.2		1.8	1.2	
Bulk spectrum 2	0	2	27.6	0.5	3	7.2	3.8	2.7	2.4	0	0.1	44	4.5		0	2.2	
Bulk spectrum 3	0.9	4.3	27.7	1.1	2.5	10.6	5.2	0	1.8	0	0.8	43.5	1.4		0	0.2	
Bulk spectrum 4	0.2	4.6	24.4	1.6	1.1	15.6	3.2	2.4	0	0	4.6	41.8	0		0	0.6	
grain 1			100														quartz
grain 2		26.2				17.4						56.4					garnet
grain 3						15.7						84.3					Fe oxide
grain 4						18.1						81.9					Fe oxide
grain 5		11	42.9			9.8						36.3					garnet
grain 6			9.4			10.1						80.5					garnet
grain 7			71									29					garnet
grain 8			25.3									74.7					garnet
grain 9			36.3			12						51.6					garnet
grain 10			34.7		31.8							33.5					pyrite
grain 11		8.6	53.9				5					32.5					garnet
grain 12			19.9			9.2						70.9					garnet
grain 13			16.6									83.4					garnet
grain 14			42.3			9.8						48					garnet
grain 15			14.4									85.6					garnet
grain 16			30.3									49.9		19.8			garnet
grain 17			30.3									69.7					garnet
grain 18			25.7									74.3					garnet
grain 19			37.8			10.4						51.8					garnet
grain 20			29			14.7						56.4					garnet

	All elements (normalized) [wt %]																
17IB06	**Mg**	**Al**	**Si**	**P**	**S**	**Cl**	**K**	**Ca**	**Ti**	**Cr**	**Mn**	**Fe**	**Zn**	**Br**	**Zr**	**Ce**	**mineral**
Bulk spectrum 1	0.7	2.7	24.4	2.2	4.2	10.8	3.1	1.3	1.2	0.7	2.2	45.7	0.7		0	0	
Bulk spectrum 2	0.3	3.3	23.3	0.6	8.9	8.7	4.6	0.8	0.7	0	0	45.3	1		2.5	0	
Bulk spectrum 3	0.3	4.1	25.8	0.6	4.1	10.9	4.1	0.8	1.3	1.8	0	39.4	3		0.9	3	
Bulk spectrum 4	0.4	3.7	23.7	0.4	5.4	10.6	3.1	1.8	0.4	0.5	2.3	37.6	4		6.1	0	
																	biotite
grain 1 [wt %]		7.4	35.7			13.2	9.1					34.5					(?)
grain 2			32.7			9.1						58.2					unknown
																	biotite
grain 3			53.2			12.1	5.3					29.4					(?)
grain 4			3.9		70.9							25.2					pyrite
																	biotite
grain 5			40.4				4.6					41.4		13.6			(?)
grain 6		2.7	75.5			3.1						18.7					
grain 7			11.9		30.4	9.8						47.9					
grain 8			75		3.7							21.3					
grain 9		6.9	50.1						7.1			35.9					
grain 10		7.6	36.6			10						45.8					
grain 11			79.6									20.4					
grain 12		6.4	61.5			4.6						27.4					garnet
grain 13		10.1	28.1									61.8					garnet
grain 14			61.8			6.2						32					
grain 15			13.8		41.9							44.3					
grain 16			34.3					13.2				11.8		40.6			garnet
grain 17		11.6	27.9			13.5	10.6					36.3					
grain 18			14.9			16.5						68.6					
grain 19		25.1	38.3			4		18.8				13.8					
grain 20		14.6	38.4									47					

All elements (normalized) [wt %]

17IB07	Na	Mg	Al	Si	P	S	Cl	K	Ca	Ti	Cr	Mn	Fe	Zn	Br	Zr	Tm	mineral
Grain 2			4.1	25			6									64.9		zircon
Grain 3				22.7			7.4									69.8		zircon
Grain 4				23.7												76.3		zircon
Grain 5			37.1	52.1			10.8											garnet
Grain 6	6.9		2.9	22.7				5.5								62		zircon
Grain 7				24.8												75.2		zircon
Grain 8			38.6	61.4														garnet
Grain 9		12.3	26.2	61.5														garnet
Grain 10				24.3												75.7		zircon
Grain 11		11.9	36	52.1														garnet
Grain 12			31.8	68.2														garnet (?)
Grain 13			15.6	31.6			16			36.8								garnet (?)
Grain 14		9.6	32.7	57.7														garnet
Grain 15				21.3			5									54.6	19.1	zircon
Grain 16				37.9												62.1		zircon
Grain 17			3.3	22.5			6									68.3		zircon
Grain 18			7.3	17.5						75.2								titanite
Grain 19				40.4			28.9								30.6			unknown
Grain 20				85.4			14.6											quartz
grain 1		9.8	35.5	54.7														garnet
Bulk spectrum 1		2.8	12.8	25.1	1.2	0.2	6.6	2.1	3	11.6	0	0	14.4	2.6		17.6		
Bulk spectrum 2		4.8	17.3	29.2	0.7	0	8.5	2.3	1.1	7.8	0	0	13.9	3.1		11.2		
Bulk spectrum 3		5.2	15.2	31.3	0	0.6	11	1.1	1.8	1.8	0	0.9	16.9	2.8		11.4		
Bulk spectrum 4		3.1	15.9	33.8	0	1.6	9	2.8	3.2	9.7	1.8	0	17.1	0		1.9		